EFFECT OF CROSSLINK DENSITY ON THE TEARING OF GUM NATURAL RUBBER CURED WITH DICUMYL PEROXIDE (DCP)

A Thesis

Presented to

The Graduate Faculty of The University of Akron

In Partial Fulfillment

of the Requirements for the Degree

Master of Science

Yanxiao Li

May, 2013

EFFECT OF CROSSLINK DENSITY ON THE TEARING OF GUM NATURAL RUBBER CURED WITH DICUMYL PEROXIDE (DCP)

Yanxiao Li

Thesis

Approved:	Accepted:
Advisor Dr. Gary R. Hamed	Dean of the College Dr. Stephen Z. D. Cheng
Faculty Reader Dr. Ali Dhinojwala	Dean of the Graduate School Dr. George R. Newkome
Department Chair Dr. Coleen Pugh	Date

ABSTRACT

The goal of the present work is to study and understand the fracture of NR vulcanized with different levels of DCP. The tensile behavior of gum natural rubber (NR) vulcanizates cured with dicumyl peroxide (DCP) was studied. The effect of crosslink density on tensile strength, tear strength, strain, 100% modulus, and the critical cut size was determined. Dumbbell specimens cured with different level of DCP with (normal tensile test) and without (tear test) edge cuts, were strained continuously to rupture. Tensile strengths refer to breaking stress for uncut specimens, while tear strengths are for specimens with precuts.

DCP-cured gum natural rubber vulcanizates with different crosslink densities (10 different amounts of curatives were added to the masterbatch) were prepared. Normal tensile and tear tests were determined. As with sulfur cured gums, the tensile strength of DCP cured gum natural rubber passes through a maximum with increased crosslink density. Breaking strain and 100% modulus show a linear relationship with the crosslink density. However, the results obtained from tear tests were quite different from those with the sulfur curing system. Log-log plots of stress at break versus cut size were made for all the vulcanizates. An unstable region is observed for the lightly and moderately crosslinked specimens; results are scattered because some of the specimens undergo bulk crystallization while others with the same cut sizes do not. Values of critical cut sizes as

well as the widths of unstable regions also showed a dependence on the crosslink density. No drop in strength could be observed in highly crosslinked specimens due to the lack of crystallization. This is like the results with sulfur curing.

ACKNOWLEDGEMENTS

I wish to express my sincere appreciation and respect to my advisor, Dr. G. R. Hamed, who is always very patient to answer all my questions. I've really learned a lot from him, not only in research but also the attitude towards life. It's my pleasure to have the opportunity to be in his group.

I'd like to thank Dr. A. Dhnojwala, as the reader of my thesis, and Dr. D. H. Reneker, who were very kind and cared about my research work.

I would like to thank the staffs of the Department of Polymer Science and the Rubber lab for their technical support and kind help.

I am deeply grateful to my parents and family members for their endless love and support in the past two years.

Many thanks I would like to give my group members, whom I often studied from, and discussed problems together with. I want to thank all my friends, with whom I can always feel happy and peaceful.

Finally, I want to thanks the life I spent in Akron in the past two years. Such a memory is a treasure for me. I will never forget this period of time, in which I really grow up.

TABLE OF CONTENTS

Page

CHAPTER

LIST OF TABLES

Table Page

LIST OF FIGURES

Figure Page

CHAPTER I

INTRODUCTION

Natural rubber (NR) has high tensile strength, high resilience, excellent dynamic properties, excellent low temperature flexibility, and low heat buildup[1]. This combination makes natural rubber essential in household and industrial applications. Tires, as one of the important rubber products, are widely used all over the world. To resist tire failure, all tires contain natural rubber compounds in the location (belt edge region) of maximum stress concentration. This is the motivation for rubber research work on natural rubber fracture. A simple tensile test of edge-cut rubber specimens is one way to examine the tearing of rubber.

Based on the studies of Dr. Rattanasom concerning the effect of crosslink density on the mechanical properties of sulfur-cured gum natural rubber vulcanizates, I studied the effect of crosslink density on tearing of DCP cured gum natural rubber. Dumbbell specimens with various crosslink densities were tested and characterized. DCP, as a kind of peroxide vulcanizer, cures natural rubber in a different mechanism from sulfur. As a result, the property of sulfur cured gum NR and DCP cured gum NR could be diverse. Their dependence on crosslink density which is an important factor strongly influences the mechanical properties was compared.

CHAPTER II

HISTORICAL REVIEW

2.1 Natural Rubber (NR)

Natural rubber has high tensile strength, high resilience, excellent dynamic properties, excellent low temperature flexibility, and low heat buildup[1]. This makes natural rubber essential in household and industrial applications.

Natural rubber is obtainable from trees, shrubs, or vines of tropical and temperate regions, but, the only important commercial source of natural rubber is the latex from the trees of Hevea brasiliensis[2].

Natural rubber has a chemical structure of essentially 100% cis-1, 4-polyisoprene unit (Figure 2.1)[2]. Its number average molecular weight ranges from 10^5 to 10^6 g/mol. Due to high stereoregularity, natural rubber undergoes crystallization when it is cooled in the unstrained state (thermal crystallization) or by straining at room temperature (strain-induced crystallization). The rate of strain-induced crystallization increases with extension, because molecular alignment increases the probability of nucleation. As strain-induced crystallization causes anisotropy, this causes the tensile strength in the direction of deformation to be greater. Rapid crystallization gives natural rubber high tensile strength and good tear resistance, even in pure gum (nonreinforced) vulcanizates[3].

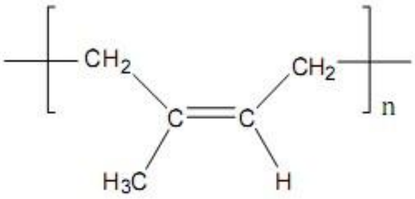

Figure 2.1 Chemical structure of natural rubber (cis-1, 4-polyisoprene)[2].

2.2 Vulcanization

Unvulcanized natural rubber is weak and does not maintain its shape if deformed due to the molecular slippage. Vulcanized rubber, on the other hand, is a three dimensional network; this enhances elasticity, strength and modulus and reduces hysteresis and plasticity.

There are various agents that will vulcanize rubber. Sulfur and organic peroxides are the most common. Sulfur is mainly used in diene rubbers, such as natural rubber, styrene-butadiene rubber and nitrile rubber. Organic peroxides are used for both saturated and unsaturated rubber[4].

2.2.1 Peroxide Vulcanization Mechanism

Peroxides can initiate polymerization, modify polymer rheology, attach functional groups through grafting, and enhance high temperature performance. Cure characteristics and vulcanizate properties depend on three main factors： the nature of the polymer, the peroxide type and concentration, and the presence of other reactive species, such as coagents[5].

Free-radicals are formed during peroxide vulcanization. The intended peroxide crosslinking reaction consists of 3 steps[5], as shown in Figure 2.2 (A, B, C): (1) Thermal decomposition of the peroxide: the oxygen-oxygen bond undergoes homolytic cleavage, yielding two radicals. (2) Hydrogen abstraction: peroxide radicals abstract hydrogen from the polymer, giving a macro-radical. (3) Cross-link formation: two polymeric radicals combine to form a covalent cross-link.

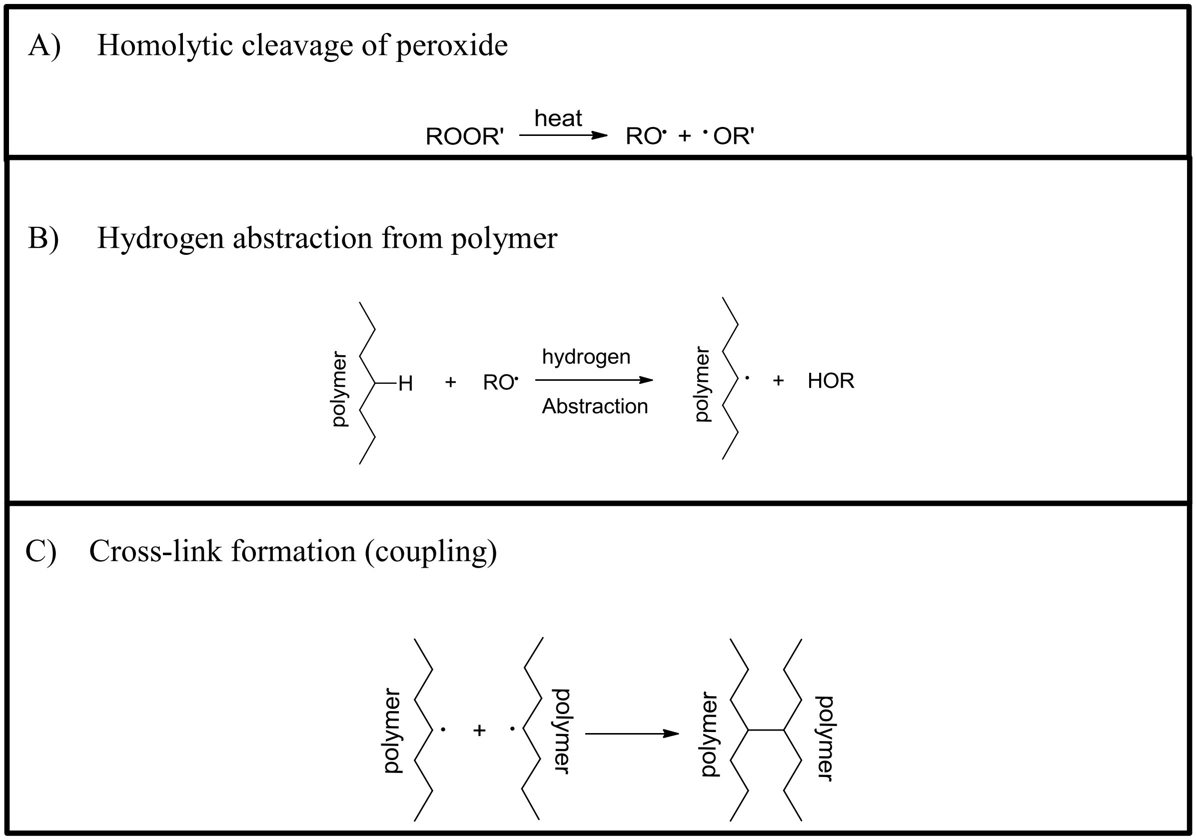
A) Homolytic cleavage of peroxide

B) Hydrogen abstraction from polymer

C) Cross-link formation (coupling)

Figure 2. 2 The basic peroxide cross-linking reaction[5].

However, in actual peroxide vulcanizations, there are side reactions that compete for the free radicals. These include beta cleavage of the oxy radical, acid-catalyzed decomposition of the peroxide, addition, radical transfer, polymer scission, dehydrohalogenation, and oxygenation. Some of these reactions decrease the final cure. Others augment cross-linking reaction by making more efficient use of radicals[5]. Curative selection and cure conditions are critical.

A. Homolytic cleavage: Peroxide decomposition is a both time and temperature depended reaction, and for dicumyl peroxide, ten minutes is needed for substantial decomposition at 150°C. *Ten-hour half-life temperature (10-h HL)* is commonly used to estimate the peroxide stability [6, 7]. The value for dicumyl peroxide is 114°C[6, 7]. So, dicumyl peroxide cures comparatively fast at a relatively lower temperature, but can be scorchy.

B. Hydrogen abstraction: The energy level of radicals determines reaction efficiency. Hydrogen abstraction proceeds only if the energy level of the radical is reduced in the process[5]. The energy level for dicumyl peroxide is 105 kcal/mol[8, 9]. This is a high value among various peroxides. Thus, its radicals can easily abstract hydrogens from other chemicals.

C. Radical coupling (cross-linking formation): This is thermodynamically favored, because of the low concentration of radical sites on the polymer and the inability of the polymers to diffuse rapidly. Thus, a small number of polymer radicals may get trapped in the crosslinked matrix and stay for months[10].

D. Beta cleavage of the oxy radical: As shown in Figure 2.3, the cumyloxy radical may undergo beta cleavage and form acetophenone and a methyl radical. This radical has a similar energy level as the cumyloxy radical. Thus, reaction efficiency may be increased because the methyl radical was less steric hinderance than the cumyloxy radical[5].

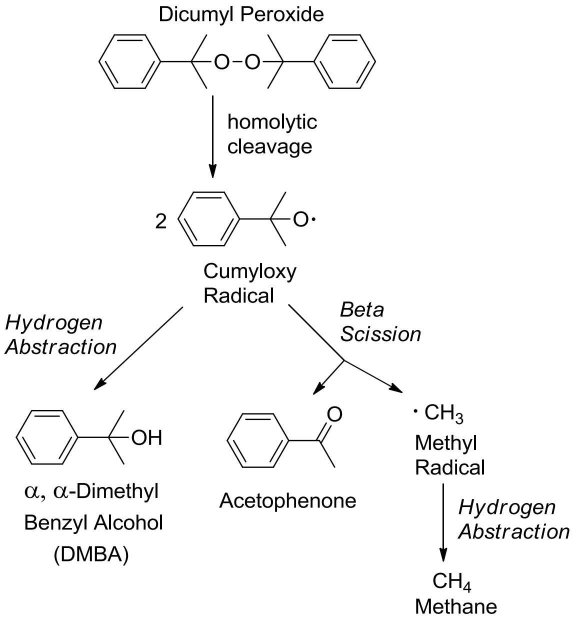

Figure 2. 3 Rearrangement (beta scission) of cumyloxy radical to yield methyl radicals[5].

E. Addition reactions: A radical fragment may attach to a double bond (Figure 2.4 (D)), thereby initiating radical fragments that are incorporated into the polymer network. Natural rubber is unsaturated and peroxide radicals can react with natural rubber by addition to its double bond and by hydrogen abstracting. Hydrogen abstraction dominates in most cases. Factors influencing the balance of abstraction and addition are polymer structure, the type and concentration of peroxide, and temperature. Peroxide efficiency influences which mechanism dominates. In abstraction reactions, one mole of peroxide can form only one mole of cross-links. In the addition mechanism, one radical can give rise to several bonds. Abstraction is dominant in peroxide/natural rubber reactions[11]. Also, higher peroxide concentrations and higher temperatures favor addition reactions[11, 12].

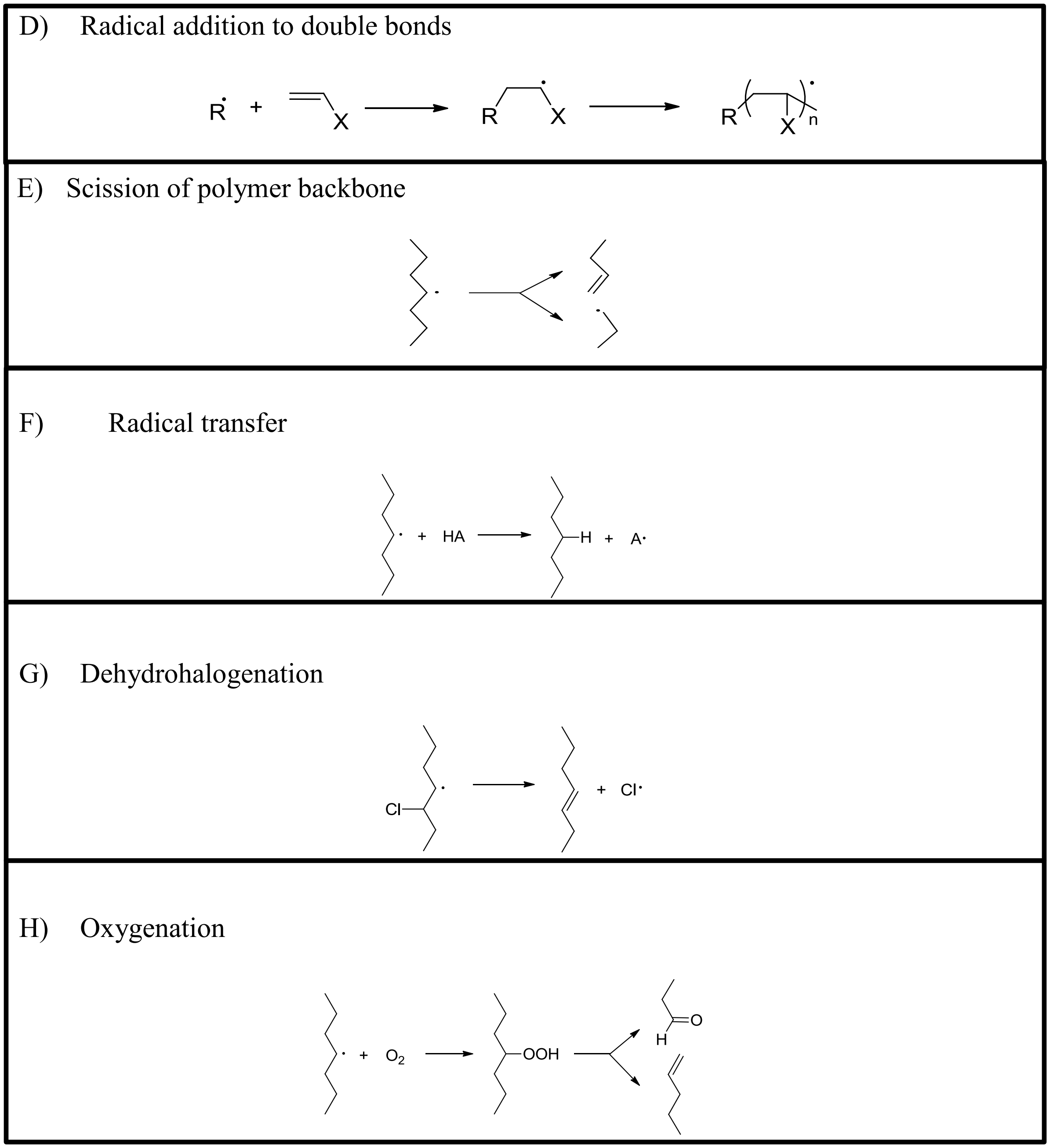

D) Radical addition to double bonds

E) Scission of polymer backbone

F) Radical transfer

G) Dehydrohalogenation

H) Oxygenation

Figure 2. 4 Competing chemical mechanisms involved in peroxide cross-linking[5].

F. Polymer scission: This reaction (Figure 2.4 (E)) reduces cross-linking. The polymer backbone breaks and gives rise to a double bond and a radical. Unsaturated and oxidation products will be included in the final vulcanizates. Polymers with a structure like polypropylene undergo scission rather than cross-linking[15-18]. Furthermore, the competition between cross-linking and scission also is affected by peroxide concentration and temperature. Scission prevails at a lower peroxide concentration system and at higher temperature[15, 19, and 20].

G. Radical transfer: as shown in Figure 2.4 (F), radical transfer often occurs between polymer radicals and chemicals with easily abstractable hydrogen atoms. When contact with readily abstractable hydrogen, the high energy radical will remove the hydrogen and form a more stable radical. This mechanism suppresses the vulcanization reaction by neutralizing polymer radicals before they form cross-links[15].

H. Oxygenation: Oxygen reacts with polymer radicals (Figure 2.4 (H)) and prevents them from forming crosslinks. Hydroperoxides that form can decompose to break the polymer backbone on heating. However, the detrimental effects of oxygen are usually only significant at the surface of a rubber. Surface tackiness is one manifestation of this phenomenon[16, 17].

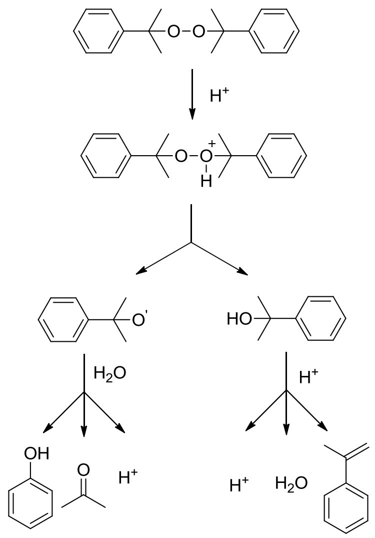

Figure 2. 5 Acid-catalyzed decomposition of dicumyl peroxide[5].

I. Acid-catalyzed decomposition of the peroxide: Dicumyl peroxide can be decomposed by strong acids (Figure 2.5). Peroxide efficiency is decreased because peroxide is consumed without radical formation. In order to prevent this problem, clay fillers and acidic carbon blacks should be avoided[16, 17].

2.2.2 Comparison of Peroxide and Sulfur Vulcanization

Cross-links produced by peroxide vulcanization are carbon-carbon bonds whose strength is similar to those in the polymer backbone. Polysulfide crosslinks generated during sulfur vulcanization are more flexible, but not as strong as carbon-carbon bonds. Peroxide vulcanized rubber exhibits lower compression set and better heat aging properties. Sulfur crosslinks are more easily broken by mechanical or thermal energy, but they result in better hot tear and abrasion resistance[5]. Additionally, sulfur cures have a longer induction period before cure. Peroxide cures have minimal induction periods and may show scorch.

Sometimes, peroxide vulcanizates have enhanced properties compared to sulfur-cured systems[16, 17]. In these cases, after heat aging, sulfur-vulcanizate exhibit large changes in percent elongation and hardness, while peroxide-cured elastomers show minimal effects[5].

2.2.3 Effect of Vulcanization on Properties of Rubber

Crosslink density has an important influence on the properties of rubber. With increased crosslinking, stiffness and elasticity increase, while hysteresis, permanent set and friction properties decrease. Tear strength, fatigue lifetime, toughness and tensile strength reach maxima at certain crosslink densities[24].

Hamed has carried out research on the effect of crosslink density on the strength of rubber[25]. Uncut specimens of filled and gum NR vulcanizates had similar strength at low crosslink density, while, at high crosslink density, gum NR vulcanizates became much weaker. At low crosslink levels, the fracture may occur via viscous flow, without breakage of chemical bonds, but fracture of chemical bonds must occur after gelation. Brittle fracture ensues if crosslink density is very high.

2.2.4 Vulcanization Parameters and formulation considerations

A cure curve shows the degree of vulcanization as a function of time and temperature. This can be measured with the Moving Die Rheometer (MDR). A cure curve is a “torque versus time (at a given temperature) plot”, as shown in Figure 2.6. The torque is a measure of shear modulus. When heating starts, torque declines, because of decreased viscosity. After vulcanization starts, torque rises rapidly due to crosslinks. Often, the final cure plateaus. There are two other types of cure curves. If crosslinking continues, torque will keep increasing (creep). If chain scission and/or crosslink breakage dominate, the curve passes through a maximum (reversion). A number of cure parameters can be read from the cure curve; scorch time t_{s2}(prior to vulcanization), optimum cure time t_{90} (typically 85 to 95% of maximum cure), and maximum cure time t_{100} (prior to over cure). To avoid over cure, it’s better to keep the initial cure slightly below the maximum. This allows leeway for some post cure[25].

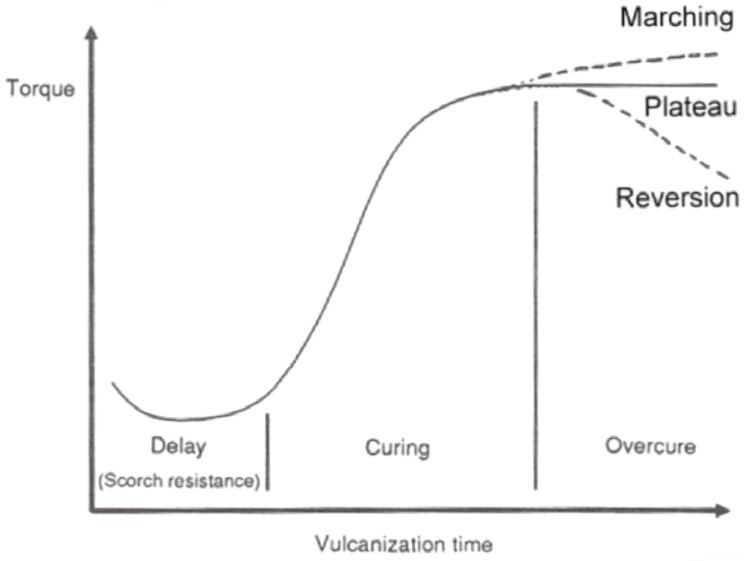

Figure 2. 6 Cure curve characteristics[25].

Rubber compounds are usually a complicated mixture of polymers, curatives, oils, antidegradants, coagents, and fillers. All may have effect on crosslinking.

A. Peroxide. The main criteria for peroxide selection should be[17]:

- an effective vulcanizer for the elastomer;
- a proper decomposition temperature to avoid scorch, but allow fast curing at the vulcanization temperature;
- not vulnerable to side reactions; additives must not catalyze oxidation or degradation of the polymer;
- Nonvolatile, nontoxic, nonirritating and safe to handle.

The concentration of peroxide is an important determinant of final properties. Increased peroxide increases crosslink density. This increases the modulus and hardness, and decreases percent elongation[26].

Dialkyl peroxides are the one most commonly used in vulcanization. DCP is non-blooming and highly reactive at medium processing and curing temperatures. The recommended cure temperature is typically 160°C[28].

B. Polymers. Some polymers can be readily crosslinked with peroxide, but others may degrade. Peroxide crosslink of unsaturated polymers is rapid because of a higher concentration of allylic hydrogens. Generally, the relative efficiency of peroxide vulcanization of polymers is shown as follows[12]:

BR > NR&SBR > NBR > CR > EPDM > EPR > CPE

Unsaturated rubbers like NR, synthetic isoprene rubber (IR), BR, and SBR (with allylic hydrogen atoms) can undergo hydrogen abstraction as well as radical addition to double bonds. Addition reactions are favored when acyl peroxides (benzoyl peroxide) are used, while dialkyl peroxides usually favor hydrogen abstraction. Higher temperatures and higher peroxide concentration shift toward the addition mechanism[12, 26, and 27].

C. Coagents. Because of the unsaturated structure in coagents, addition/polymerization is the principal mechanism for coagents/rubber reactions. Coagents improve physical properties and processability of peroxide-cured elastomers. Heat aging resistance, higher modulus, and higher tensile strength, higher tear strength, higher hardness, increased abrasion resistance, improved abrasion resistance, improved resilience, lower Mooney viscosity and improved rubber/medal adhesion are seen[16].

D. Antidegradants. Oxidation is the main cause of degradation in natural rubber. This is a radical process that takes place when carbon-carbon bonds break to form radicals. Oxidation is accelerated when a natural rubber compound is exposed to light, heat or mechanical stress. As shown in Figure 2.4 (H), polymer radicals are converted to hydroperoxides and eventually decompose to polymer radicals in a cascading cycle. This is detrimental to the vulcanizates[16, 17]. Antioxidants function by neutralizing oxy or polymer radicals before they can degrade the polymer, but at the same time, they can interfere with peroxide vulcanization. As a result, certain antioxidants are recommended. PANA is phenyl-α-naphthylamine, which is a powerful general-purpose antioxidant that is also an anti-flexcracking agent. In a general rubber compound, 1.0-2.0 phr of this antioxidant is recommended.

E. Oil extenders. Paraffinic oils have the least effect on peroxide efficiency. Aromatic oils should be avoided because they strongly inhibit peroxide curing[16, 17].

F. Fillers. Some fillers cause acid-catalyzed decomposition of the peroxide. This will severely decrease peroxide efficiency. Thus, acidic fillers should be avoided[16, 17].

During vulcanization the temperature should not be too high, because rapid generation of gaseous vulcanization by-products to escape may produce bubbles. Air should be excluded during peroxide vulcanization, since oxygen is detrimental to crosslinking[5].

2.2.5 Determination of Crosslink Density

The most important characteristic of an elastomeric network is its density of crosslinking [29, 30, 31]. There are two common methods to measure crosslink density: swelling equilibrium and stress-strain measurements.

Vulcanized rubber does not dissolve in solvent; instead it swells. The Flory-Rehner equation can be used to calculate the crosslink density, ρ_c[32, 33]:

$$\rho_c = -\frac{\ln(1-v_r)+v_r+\chi v_r^2}{2v_s\left(v_r^{\frac{1}{3}}-\frac{v_r}{2}\right)} \tag{2.1}$$

where ρ_c = crosslink density (moles of crosslinks per unit volume); v_r = volume fraction of rubber in the swollen gel; v_s = molar volume of the swelling solvent; χ = interaction parameter of the solvent and rubber.

Another way to determine the crosslink density is to use the Mooney-Rivlin equation[34] to interpret stress-strain data:

$$\frac{\sigma}{2(\lambda-\lambda^{-2})} = C_1 + \frac{C_2}{\lambda} \tag{2.2}$$

where σ = stress obtained from stress-strain measurements at equilibrium; λ = extension ration obtained from stress-strain measurements, which represents elongation; $C_1 = \rho_c RT$, which stands for elastic modulus; ρ_c = crosslink density (moles of crosslinks per unit volume); R = gas constant; T = temperature.

The left hand side of Equation 2.2 is plotted as a function of the reciprocal elongation, and C_1 and C_2 are determined.

2.3 Fracture of Rubber

Vulcanizates are inhomogeneous, containing flaws of various shapes and sizes. When a solid is subjected to a global stress, the local stress is magnified; often, this stress is many times larger than the applied stress. Fracture initiates from a flaw where stress magnification is greatest. Fracture is a process in which network chains are broken and new free surface is created[35, 36, 37].

2.3.1 Fracture Mechanics

Two methodologies have been often used to evaluate fracture: the critical stress criterion and the energy balance criterion.

The region near a flaw undergoes larger local stress and strain than global values. Fracture will occur by a catastrophic dissociation of backbone bonds at the critical local stress that causes crack propagation[38]. Inglis[35] showed that the local stress σ_t and the global stress σ are related:

$$\sigma_t = \sigma\,[1 + 2(l/r)^{1/2}] \qquad (2.3)$$

where l = depth of the edge flaw; r = radius of the flaw tip.

The flaw length is usually larger than the radius of the tip, so that this equation can be simplified to:

$$\sigma_t = 2\sigma\,(l/r)^{1/2} \qquad (2.4)$$

Long, sharp flaws give large local stresses, which promote fracture. Stress concentration at the tip of a flaw must be reduced to delay fracture.

Energy conservation is another way to analyze fracture. An energy balance can be expressed as[12]:

$$\Delta W_S + \Delta W_P = G\ (\Delta A) + \Delta W_e \qquad (2.5)$$

where ΔW_S = stored strain energy released from the bulk when a crack grows; ΔW_P = change of energy from the loading machine when a crack grows; G = the fracture energy per unit area; ΔA = newly created surface due to the growth of the crack; ΔW_S = stored strain energy gained as a result of crack growth.

This equation describes the balance between the strain energy of the bulk and the surface energy resulting from the presence of a crack. Before macroscopic fracture occurs, much chain breakage takes place. If the crack tip becomes blunted during deformation or if the local stress is borne by other molecular chains, stress will be distributed near a flaw and stress concentration will be reduce, and then fracture will be inhibited.

To strengthen a network, reduction of stress concentration, i.e., increasing the uniformity of loading among network chains is needed. Two molecular mechanisms are active in this phenomenon. When an overloaded chain in a network breaks irreversibly, the load then will be carried by its neighboring chains and the elastic energy of the broken chain is dissipated into heat. This is *catastrophic energy dissipation*. With this mechanism, local network damage is permanent and the chain bears no load after rupture. On the other hand, if highly stressed chains could become less loaded, by reattaching to the network after breaking, the chain load will be more uniform. This energy dissipative process is designated *non-catastrophic energy dissipation*. This explains the higher strength of sulfur-cured vulcanizates compared to peroxide cured ones. Polysulfidic linkages are weaker than the carbon-carbon crosslinks formed by curing with peroxides. But, the sulfur-cured networks are stronger, because polysulfidic linkages can break and reform when overloaded[38].

An energy criterion for crack growth was given by Rivlin-Thomas[36]:

$$\sigma_b = \left(\frac{GE}{kc}\right)^{1/2} \tag{2.6}$$

where σ_b = stress at break; G = fracture energy as mentioned above; E = Young's modulus; k = a function which is approximately $\pi(1 + \varepsilon_b)^{-1/2}$ (ε_b is the strain at break); c = cut size (see Figure 2.7).

This equation is applicable for samples with only one crack. Also, when a critical breaking stress is achieved, a crack suddenly grows across the sample.

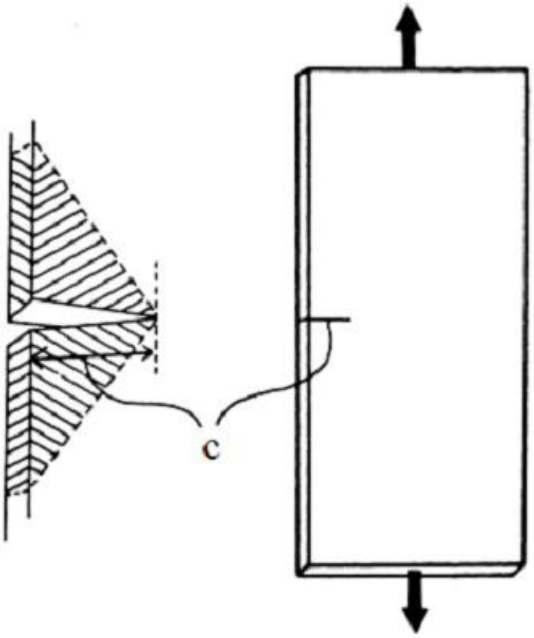

Figure 2. 7 Simple tensile specimen with edge cut length c[37].

2.3.2 Effect of Edge-cut on the Fracture of Rubber

Strain-crystallizable elastomers, such as natural rubber, have high tensile strength even without the addition of particulate filler. The high tensile strength comes from the substantial energy dissipation associated with strain-crystallization[38].

According to Rivlin-Thomas (Equation 2.6), the breaking stress of an edge-cut specimen under simple tensile stress should be proportional relationship to $c^{-1/2}$.

Strain-crystallizing natural rubber does not obey this. Thomas and Whittle[39] studied the relationship between σ_b and c using tensile tests on two peroxide-cured natural rubber vulcanizates. The tensile strength decreased with increased c. An abrupt drop in σ_b at a critical size was observed (Figure 2.8). This was attributed to bulk crystallization prior to crack propagation when $c<c_{cr}$, but the absence of bulk crystallization when $c>c_{cr}$. Critical cut size decreased with an increase of modulus.

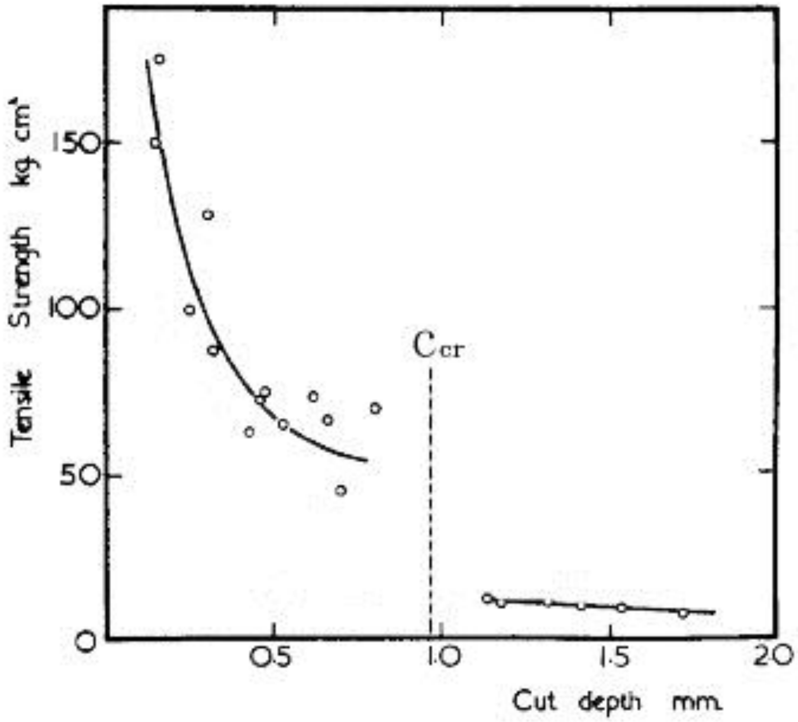

Figure 2. 8 Effect of edge-cut on tensile strength of gum natural rubber[39].

2.3.3 Effect of Crosslink Density on Edge-cut Gum (unfilled) Natural Rubber

Highly crosslinked natural rubber specimens obey Equation 2.6 and cracking is simple. But, the lightly crosslinked specimens do not follow this equation.

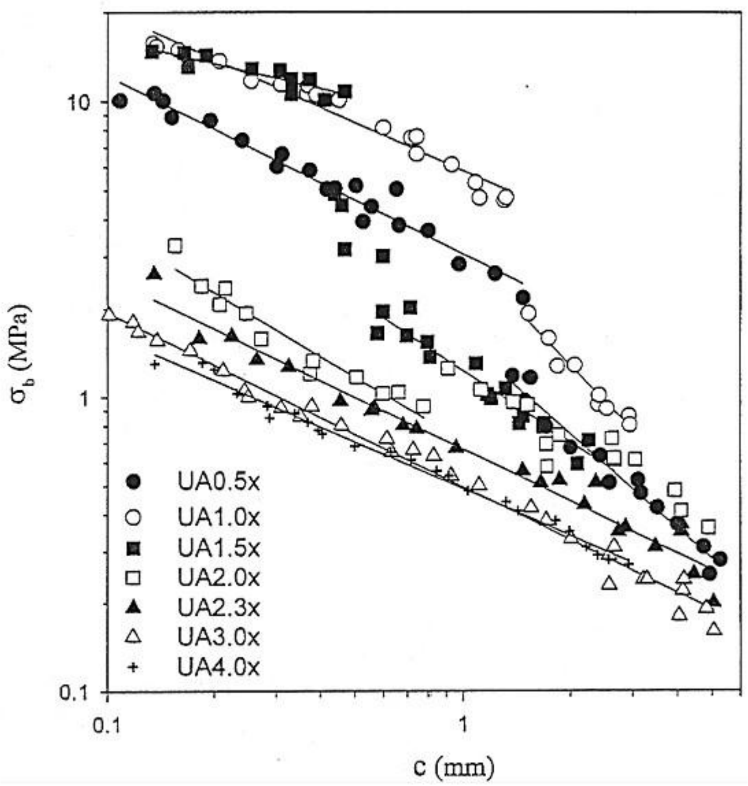

Figure 2. 9 Effect of an edge-cut on the tensile strength of gum natural rubber with different crosslink densities[40]. (UA0.5x means 0.5 times the reference level of curative in UA 1.0X; similarly for other samples.)

Hamed and Rattanasom[40] studied the effect of crosslink density on edge-cut gum natural rubber specimens vulcanized by sulfur (Figure 2.9). Dumbbell test pieces with and without edge precuts were tested in uniaxial tension. Relative strengths of different vulcanizates depended on cut size[40]. An abrupt drop in strength at a critical cut size c_{cr} was observed in lightly crosslinked natural rubber, and the crack growth showed a simple smooth surface. With increasing crosslink density, c_{cr} became smaller, and this was ascribed to reduced strain-crystallization. For highly crosslinked natural rubber, there was no c_{cr} and the lateral crack surface was rough. Crack deviation prior to rupture was observed in a moderately crosslinked composition. This specimen exhibited an unexpected slight increase in strength with increasing cut size. It was concluded that the crystallizability of natural rubber passes through a maximum with crosslink density. A small amount of crosslinking improves chain alignment under deformation, but too many crosslink junctions disrupt the structural regularity needed for crystallization.

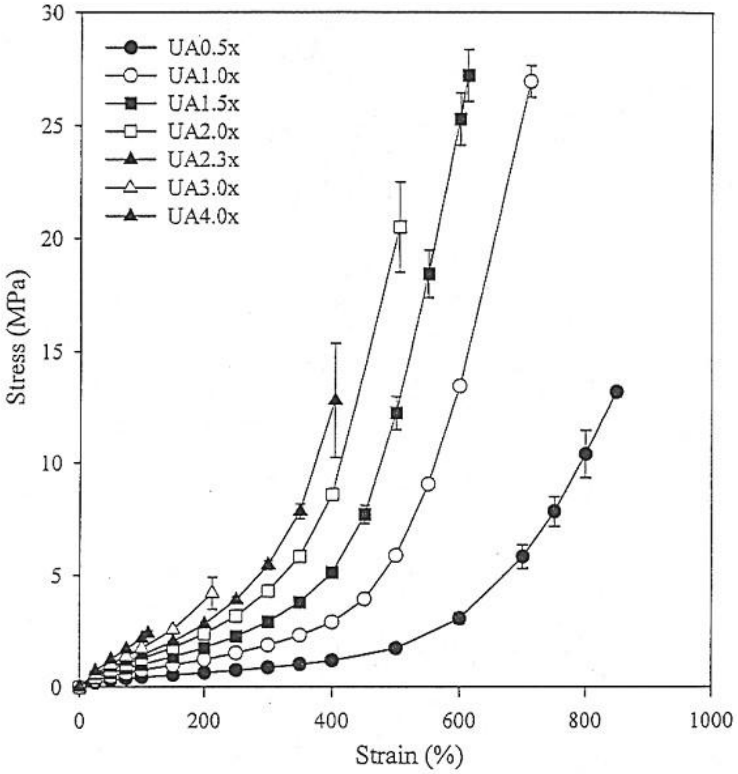

Figure 2. 10 Stress-stain curves for gum natural rubber with different crosslink densities[40].

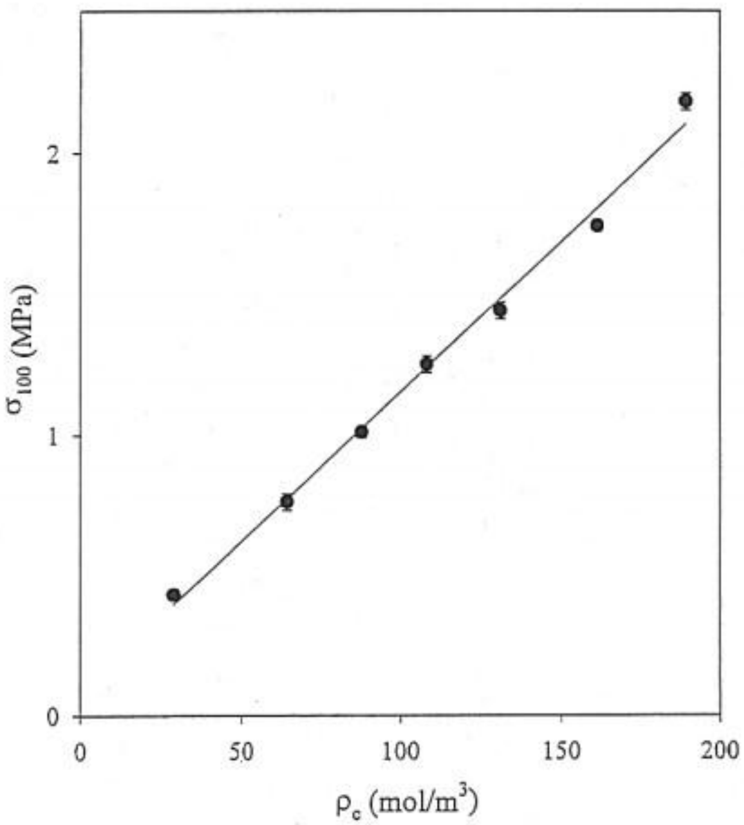

Figure 2. 11 Correlation between 100% modulus and crosslink density.

Stress-strain curves (Figure 2.10) show that ultimate elongation decreases monotonically with increasing crosslink density, while the tensile strength shows a maximum. UA1.0x and UA1.5x are stronger than the other compositions. But the highest crosslink density has a low tensile strength. This is evidence that the highly crosslinked gum natural rubber does not crystallize prior to rupture. The 100% modulus (Figure 2.11) increases linearly with the crosslink density, as expected from the simple kinetic theory of rubber elasticity

CHAPTER III

EXPERIMENTAL

3.1 Materials

1. Elastomer:
   - Natural Rubber, SMR CV-60 (Harwick Standard Distribution Corporation).
2. Antioxidant
   - Phenyl-alpha-naphthylamine, PANA powder (Akrochem Corporation).
3. Curing agent
   - Dicumyl Peroxide, DCP (Akrochem Corporation).
4. Solvent
   - Toluene, $C_6H_5CH_3$ (Fisher Scientific).

3.2 Compound Formulations

The formulations for studying the effect of crosslink density given in Table 3.1 are simple. Only natural rubber, curative DCP and antioxidant PANA are used. The designation “GD” indicates gum NR cured with DCP, and the numbers that follow the first two letters indicate the amount to curatives. For example, GD0.5 contains 0.5 phr curative DCP.

Table 3. 1 Gum (unfilled) NR formulations for varying crosslink density.

Material (phr)	GD 0.5	GD 1.0	GD 1.55	GD 1.8	GD 2.0	GD 2.5	GD 3.0	GD 4.0	GD 5.0	GD 6.0
NR (SMR CV-60)	100	100	100	100	100	100	100	100	100	100
PANA	2	2	2	2	2	2	2	2	2	2
DCP	0.5	1.0	1.55	1.8	2.0	2.5	3.0	4.0	5.0	6.0

Table 3. 2 Mixing procedure in the internal mixer.

Time (min)	Procedure
0	NR
4	PANA
8	Dump

3.3 Compounding

3.3.1 Internal Mixing

Masterbatches were prepared in a 387cc Brabender internal mixer (fill factor is 70%); the rotor speed was 50 rpm at a mixer temperature of 55 ℃. The highest torque of the rotor during mixing was less than 240 Pascal. Mixing procedures of gum Masterbatches are shown in Table 3.2. First the SMR CV60 natural rubber, cut into small pieces (about 2cm × 2cm), was mixed for 4 minutes before adding the PANA and mixing for another 4 minutes. After the torque reached a plateau (usually 8 minutes for the whole process), the mixer was stopped and the masterbatch was dumped.

3.3.2 Milling

The next step was curative addition on a two-roll mill (Farrel, 15 cm diameter and 30 cm length). Roll speeds were 8 rpm for the slow roll and 12 rpm for the fast roll. The masterbatch was masticated for about 1 minute to form a continuous sheet on the rolls, then DCP was slowly added (the roll was stopped when adding DCP to prevent it from spilling out), with alternating cuts on both sides. The masterbatch was mixed well after 3 minutes and 8 end-roll passes were made before sheeting off. The sheet was covered with two plastic films and stored at room temperature for overnight before using further.

Table 3. 3 Milling procedure on the two-roll mill.

Duration (min)	Procedure
1	Masterbatch masticated to form a continuous sheet
3	Add curing agent DCP
-	8 end-roll passes. Sheet off.

3.4 Cure Rheometry

Cure characteristics at 150 °C were determined by using a Moving Die Rheometer (MDR) equipped with the Advanced Polymer Analyzer (APA) 2000. A small piece of the compound (about 5g), between two plastic films, was placed between a pair of heating dies. The total cure time t_{100} was taken as 100 minutes.

3.5 Molding

Unvulcanized sheets (about 70 × 70 × 1 mm, about 10g) were placed in the center of a mold with 4 cavities (each cavity, 130 × 130 × 0.5mm); the rubber were sandwiched between 2 Mylar films (140 × 140 mm) and two smooth stainless steel backing plates. Samples were vulcanized at 150 ℃ for time (t_{90} + 5) min in a Dake hydraulic press. Dumbbell-shape specimens (6.35mm wide and 40mm long at the middle part) were cut from the cured sheets (about 0.6 mm thick) along the mill direction using type C die in accordance with ASTM D412 and stored at room temperature overnight before testing.

3.6 Tensile Testing

Testpieces were divided into two groups for the following tests:

1. Normal tensile tests: Normal uncut specimens were prepared for test. Specimen thickness was measured with a thickness gauge (± 0.005 mm). Extensometers were set 25 mm apart on the neck of uncut dumbbells. Tensile tests were conducted at room temperature (about 20 ℃) by an Instron (Model 5567) at a rate of 50mm/min. For each composition, five specimens were tested.

2. Tear tests: An edge-cut was made with a sharp razor blade midway along each specimen (cut size ranged from 0.1-3mm). Test conditions were the same as those used in normal tensile tests.

3.7 Swelling Test

Ten pieces cut from a cured sheet of each composition (about 0.2g each piece) were divided into two groups and each group immersed in a 40 ml vial filled with toluene in the dark at room temperature for one week. Swollen pieces were then blotted with a paper towel and immediately weighed. Then, the pieces were weighed again after drying in a vacuum oven at room temperature overnight. Crosslink density was calculated from the swollen weight and dried weight using the Flory-Rehner equation (Equation 2.1):

$$\rho_c = -\frac{\ln(1-v_r)+v_r+\chi v_r^2}{2v_s(v_r^{\frac{1}{3}}-v_r/2)} \tag{3.1}$$

where ρ_c is the crosslink density (mol/m^3); v_s is the molar volume of the swelling solvent toluene (1.07×10^{-4} m^3/mol at 25℃[41]); χ is the interaction parameter for toluene/rubber (0.39 for gum NR[41]). v_r is the volume fraction of rubber in the swollen gel, which is given by the following equation:

$$v_r = V_R/(V_R + V_S), \tag{3.2}$$

where V_R is the volume of rubber matrix; V_S is the volume of solvent; V_R and V_S are given by the following equations:

$$V_R = \frac{W_{dry}}{\rho_{dry}} \tag{3.3}$$

$$V_S = (W_{gel} - W_{dry})/\rho_{toluene} \tag{3.4}$$

where ρ_{dry} is 0.92 g/ml and $\rho_{toluene}$ is 0.862 g/ml.

3.8 Scanning Electron Microscopy (SEM)

Ruptured specimens were cut into small size and mounted on a cylindrical aluminum holder and coated with palladium before examined by scanning electron microscopy (SEM) JEOL JSM7401F. High magnification photographs of crack patterns were obtained.

CHAPTER IV

RESULTS DISCUSSION

4.1 Crosslink Density of DCP Cured Gum NR Vulcanizates

Crosslink densities of gum NR vulcanizates obtained from swelling tests are shown in Table 4.1. Figure 4.1 shows the relationship between crosslink density and the amount of curing agents. Crosslink density increases linearly with the amount of curatives.

Table 4. 1 Crosslink density of gum NR vulcanizates.

Vulcanizates	Crosslink density (mol/m^3)*
GD0.5	10.4 ± 0.5
GD 1.0	26.7 ± 0.7
GD 1.55	34.2 ± 0.8
GD 1.8	40.8 ± 1.7
GD 2.0	43.1 ± 1.2
GD 2.5	49.5 ± 1.7
GD 3.0	63.7 ± 6.9
GD 4.0	80.0 ± 6.1
GD 5.0	101 ± 6
GD 6.0	112 ± 4

*average of 10 samples.

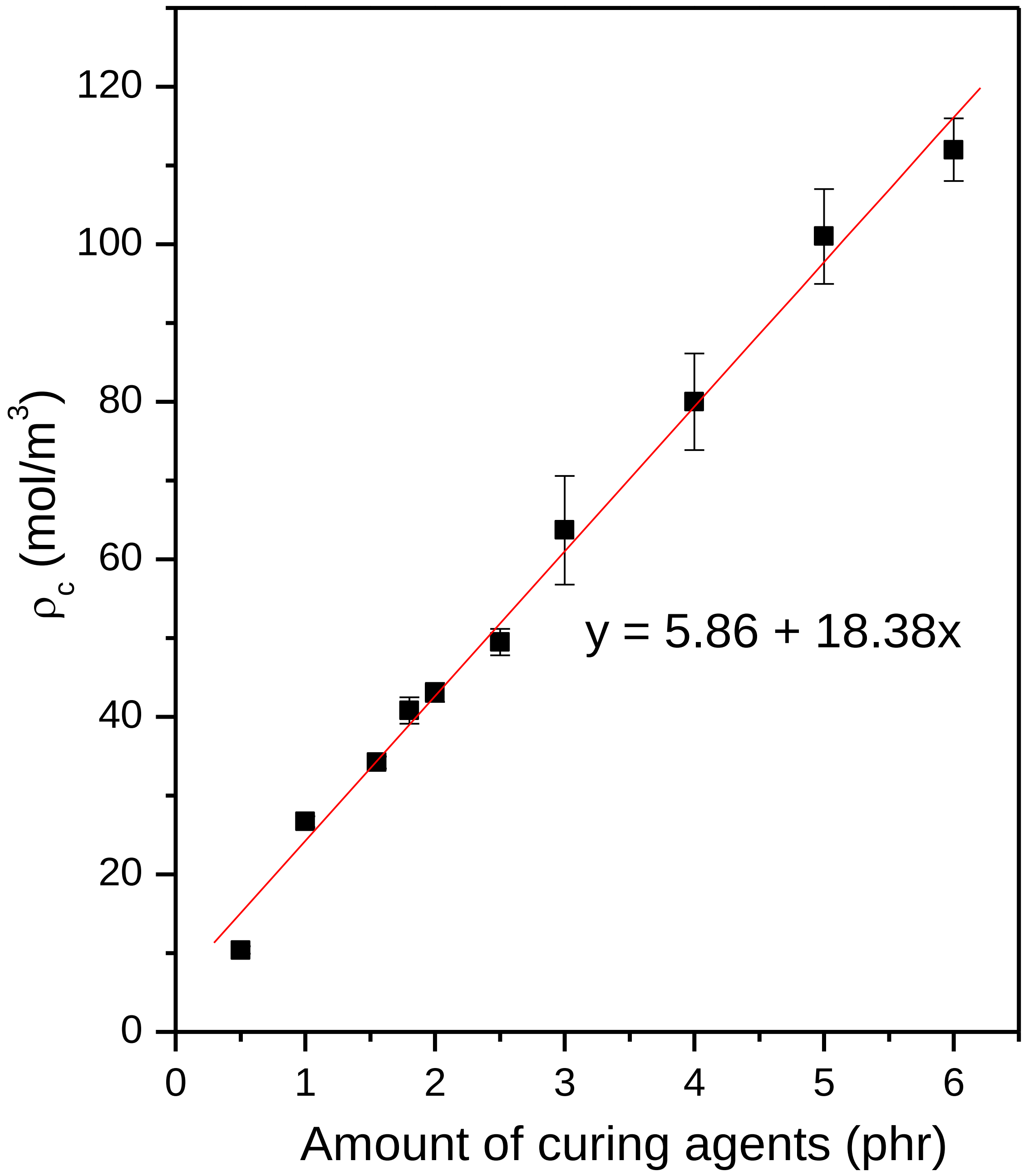

Figure 4. 1 Crosslink densities of DCP cured gum NR vulcanizates versus the amount of curatives (phr).

4.2 Vulcanization Characterization

Cure characteristics at 150℃ for the DCP cured gum NR vulcanizates are shown in Table 4.2. The definition of t_{s2} and t_c (90) are given below Table 4.2. Scorch time decreases from GD1.0 to GD6.0. No valid t_{s2} value was obtained for GD0.5 for the reason that the torque could not reach a value 2 dNm above minimum value. The optimum cure times are similar for these compounds. The minimum torque M_L shows little dependence on the amount of curatives. Maximum torques increases with increasing amount of curatives. Cure curves for all the vulcanizates are shown in Figure 4.2. All compositions start curing quickly (short scorch time). But without accelerator in the composition, torque increases slowly; which means curing process is slow. From lower crosslink density to higher crosslink density, all compositions show slight creeping phenomenon. This indicates that crosslinking continues slowly with prolonged cure. As the curves change quite slowly after 100min, sheets for tensile testing were cured to t_{90}+5. Log-log plot of the cure curves are made in Figure 4.3. It is more obvious in Figure 4.3 that the minimum torque M_L does not show the same behavior as the maximum torque $M_{HF.}$ Figure 4.4 and 4.5 shows the effect of crosslink density on scorch time t_{s2} and maximum torque $M_{HF.}$ Scorch time decreases quickly at small crosslink density, then levels off with the increase of the crosslink density. The maximum torque shows a simple linear relationship with crosslink density. Equation for the fitting line is given in the figure.

Table 4. 2 Cure Characteristics of DCP cured gum NR (150°C).

Vulcanizates	t_{s2}[a] (min)	t_c (90)[b] (min)	Minimum torque M_L(dNm)	Maximum torque M_{HF}(dNm)
GD0.5		53.2	0.73	2.14
GD 1.0	64.4	51.1	0.73	2.84
GD 1.55	23.0	52.1	0.88	3.84
GD 1.8	17.5	53.7	0.72	4.27
GD 2.0	15.0	53.0	0.60	4.53
GD 2.5	12.0	53.7	0.76	5.08
GD 3.0	10.5	55.3	0.68	5.74
GD 4.0	7.83	56.2	0.65	7.04
GD 5.0	6.56	58.0	0.66	8.45
GD 6.0	5.57	58.7	0.68	9.33

[a] t_{s2}: scorch time (time for torque to raise 2 dNm above minimum value).

[b] t_c (90): optimum cure time (time for torque to reach torque M_{90}, $M_{90} = M_L + 0.9(M_{HF} - M_L)$)

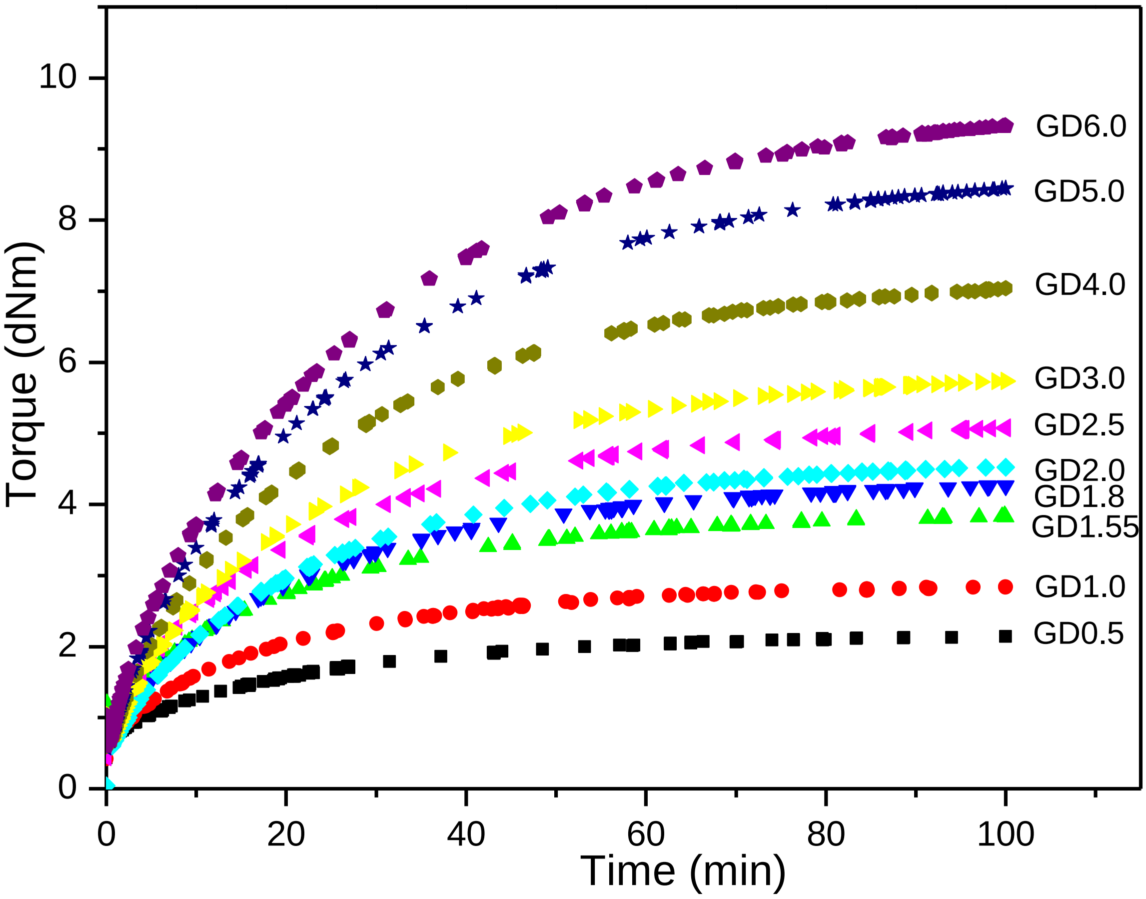

Figure 4. 2 Cure curves of DCP cured gum NR vulcanizate (150 ℃).

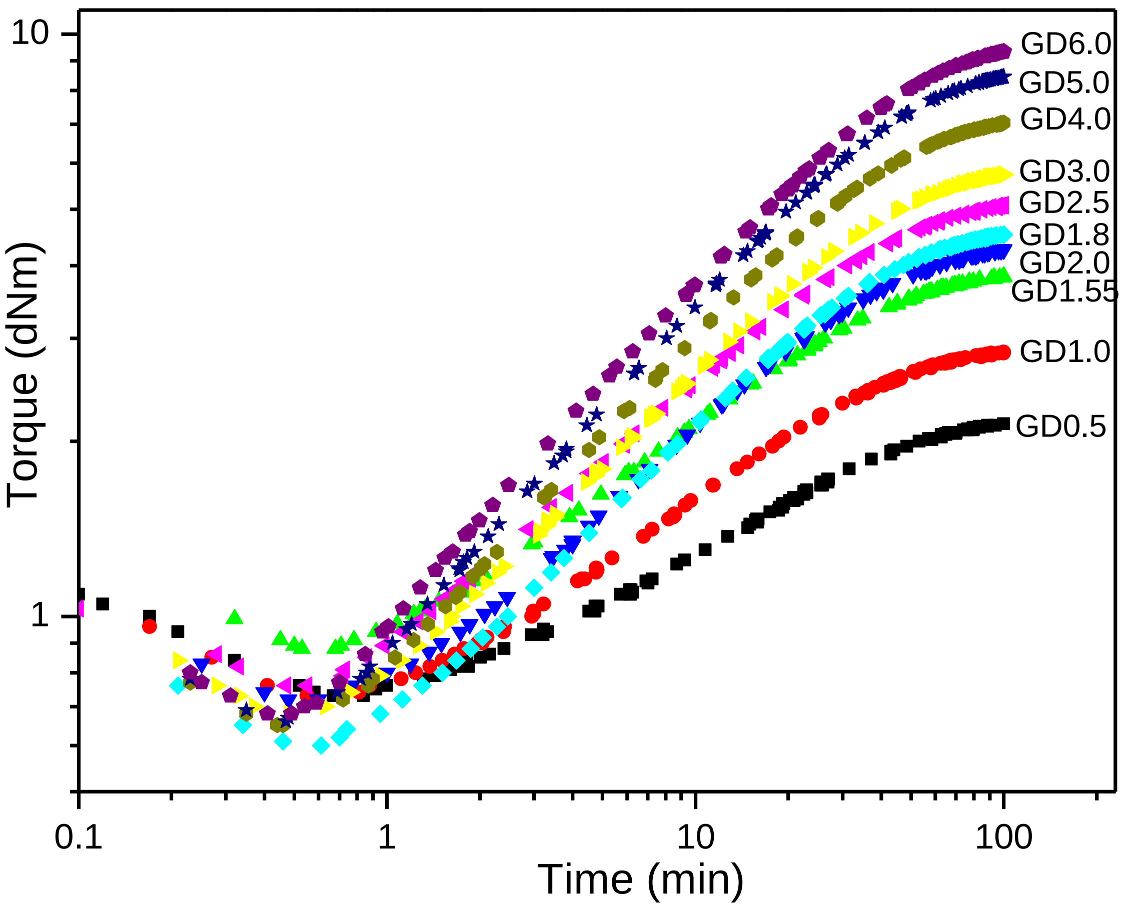

Figure 4. 3 Log-log cure curves of DCP cured gum NR vulcanizate (150 ℃).

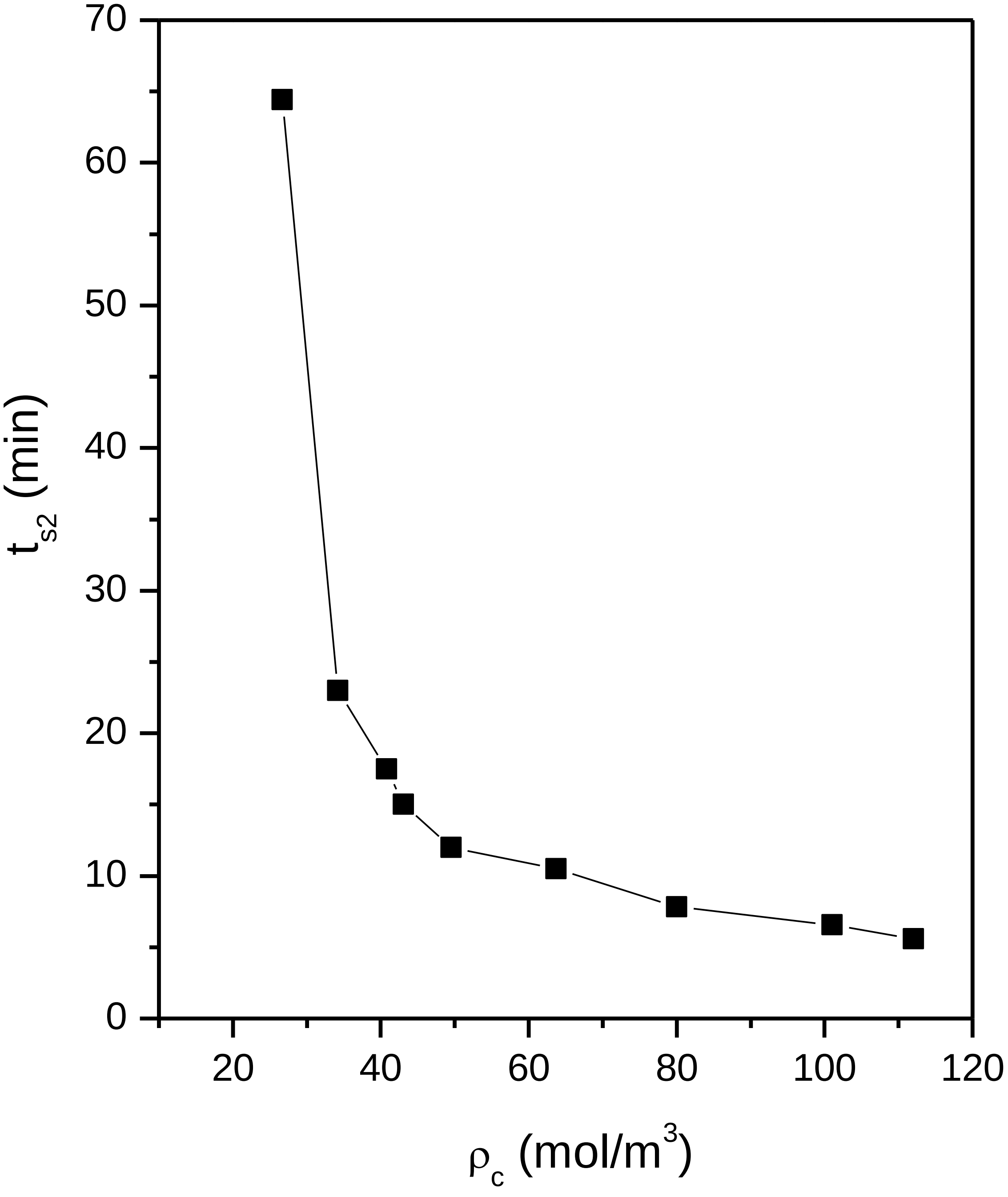

Figure 4. 4 Effect of crosslink density on scorch time ts2.

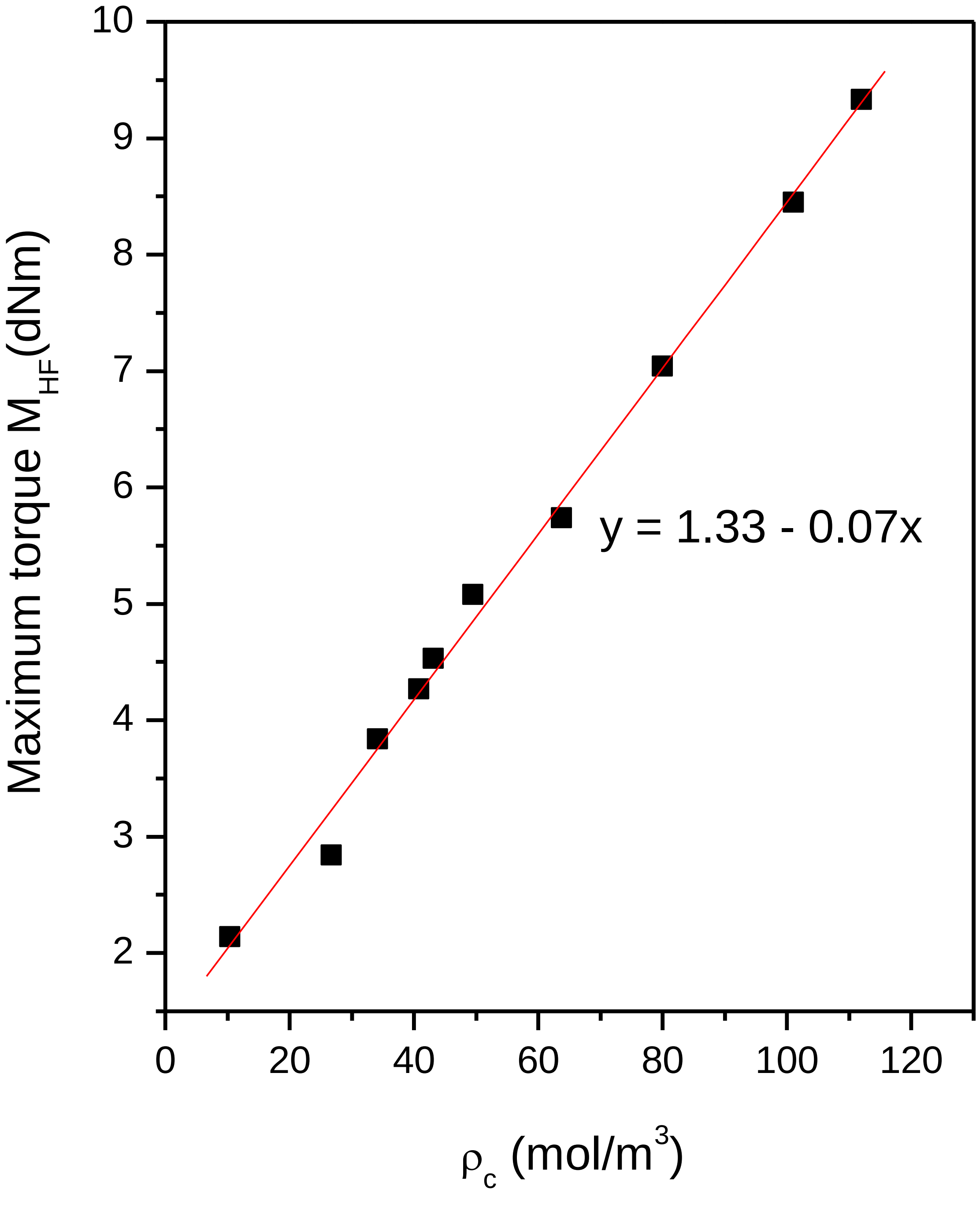

Figure 4. 5 Effect of crosslink density on maximum torque MHF.

4.3 Normal Tensile Test Results of DCP Cured Uncut Gum NR Vulcanizates

Table 4.3 shows the normal tensile test results for all the 10 vulcanizates from GD0.5 to GD6.0. Stress-strain curves of all the uncut specimens, obtained from normal tensile test, are given in Figure 4.6.

Tensile strength, as the breaking stress for the uncut specimen, initially increases with crosslink density, then decreases after passing through a maximum at GD3.0. Tensile strength versus crosslink density of DCP cured gum NR vulcanizates is plotted in Figure 4.7. For the under crosslinked vulcanizates, GD0.5, similar to those uncrosslinked, chains may readily slide past one another and disentangle, like viscous flow, fracture occurs without breaking chemical bonds, so its tensile strength is low. With the increase of crosslink density, more crosslinks formed and it becomes difficult for chains to disentangle, which results in the increase of the tensile strength. When there is sufficient crosslinks, gel point is reached, at which a gel which could not be fractured without breaking chemical bonds is formed. At this point parts of the input energy are dissipated into heat through molecular motions, leading to less energy for breaking chains to cause fracture[43]. So tensile strength is higher at this gel point. While for the highly crosslinked, chain motions are restricted and energy is incapable of dissipating. Brittle fracture occurs and specimens break with lower tensile strength[44]. Furthermore, network chains of highly crosslinked samples are shorter than those with less crosslinked samples thus they reach finite extensibility faster and exhibit lower breaking strain[44]. That the reason for the decrease of the ultimate elongation with increasing crosslink density (Figure 4.8).

The 100% modulus is the stress of uncut rubber specimens at 100% deformation, which represents stiffness. 100% modulus as a function of crosslink density is plotted in Figure 4.9. Stiffness increases monotonically with crosslink density.

Table 4. 3 tensile properties of Uncut gum NR vulcanizates

Vulcanizates	Property		
	Tensile strength σ_{b0} (MPa)	Ultimate elongation ε_{bo} (100%)	100% mod. (MPa)
GD0.5	2.87 ± 0.00	8.51 ± 0.00	0.26 ± 0.00
GD 1.0	6.15 ± 0.00	7.64 ± 0.00	0.35 ± 0.00
GD 1.55	7.06 ± 0.56	6.73 ± 0.20	0.45 ± 0.02
GD 1.8	8.84 ± 1.58	6.51 ± 0.20	0.50 ± 0.01
GD 2.0	11.1 ± 1.4	6.45 ± 0.18	0.54 ± 0.03
GD 2.5	12.9 ± 1.0	6.18 ± 0.20	0.61 ± 0.02
GD 3.0	17.3 ± 1.4	6.11 ± 0.20	0.69 ± 0.02
GD 4.0	16.3 ± 1.4	5.18 ± 0.21	0.88 ± 0.03
GD 5.0	14.4 ± 2.0	4.45 ± 0.25	1.06 ± 0.05
GD 6.0	11.5 ± 1.6	4.03 ± 0.13	1.14 ± 0.04

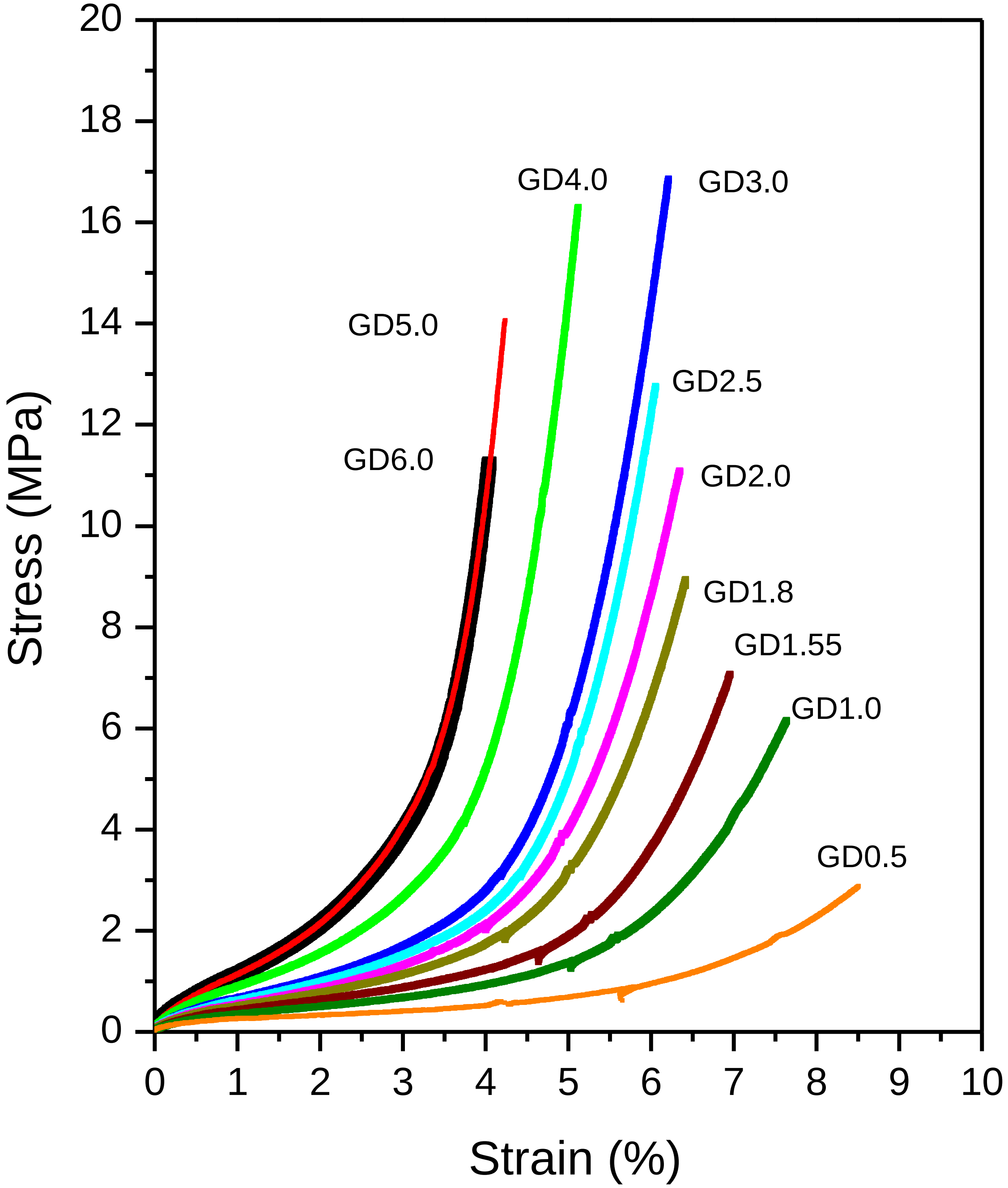

Figure 4. 6 Stress-strain curves of uncut DCP cured gum NR vulcanizates with various crosslink densities.

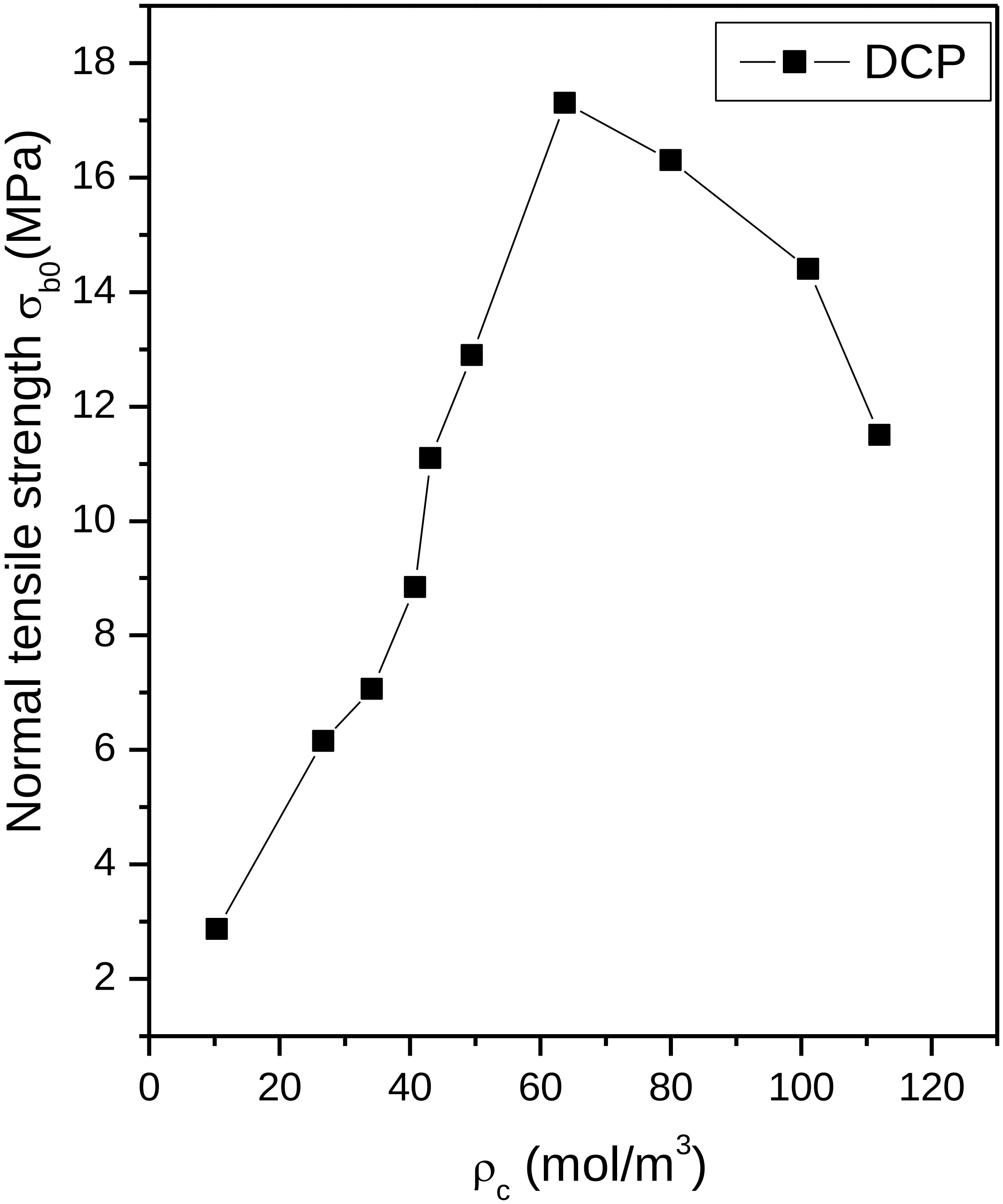

Figure 4. 7 Normal tensile strength b0 versus crosslink density of DCP cured gum NR vulcanizates.

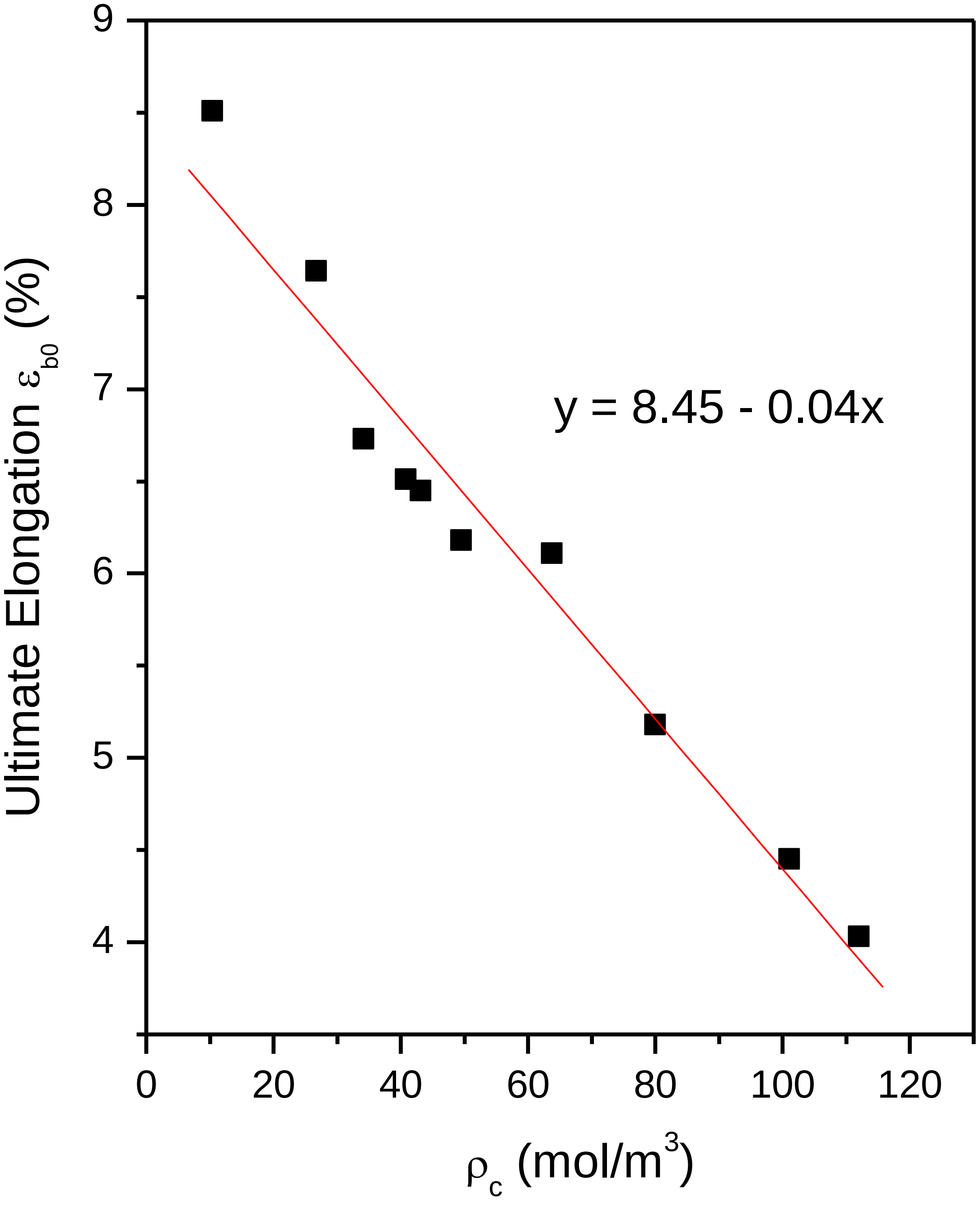

Figure 4. 8 Ultimate elongation bo versus crosslink density of DCP cured gum NR vulcanizates.

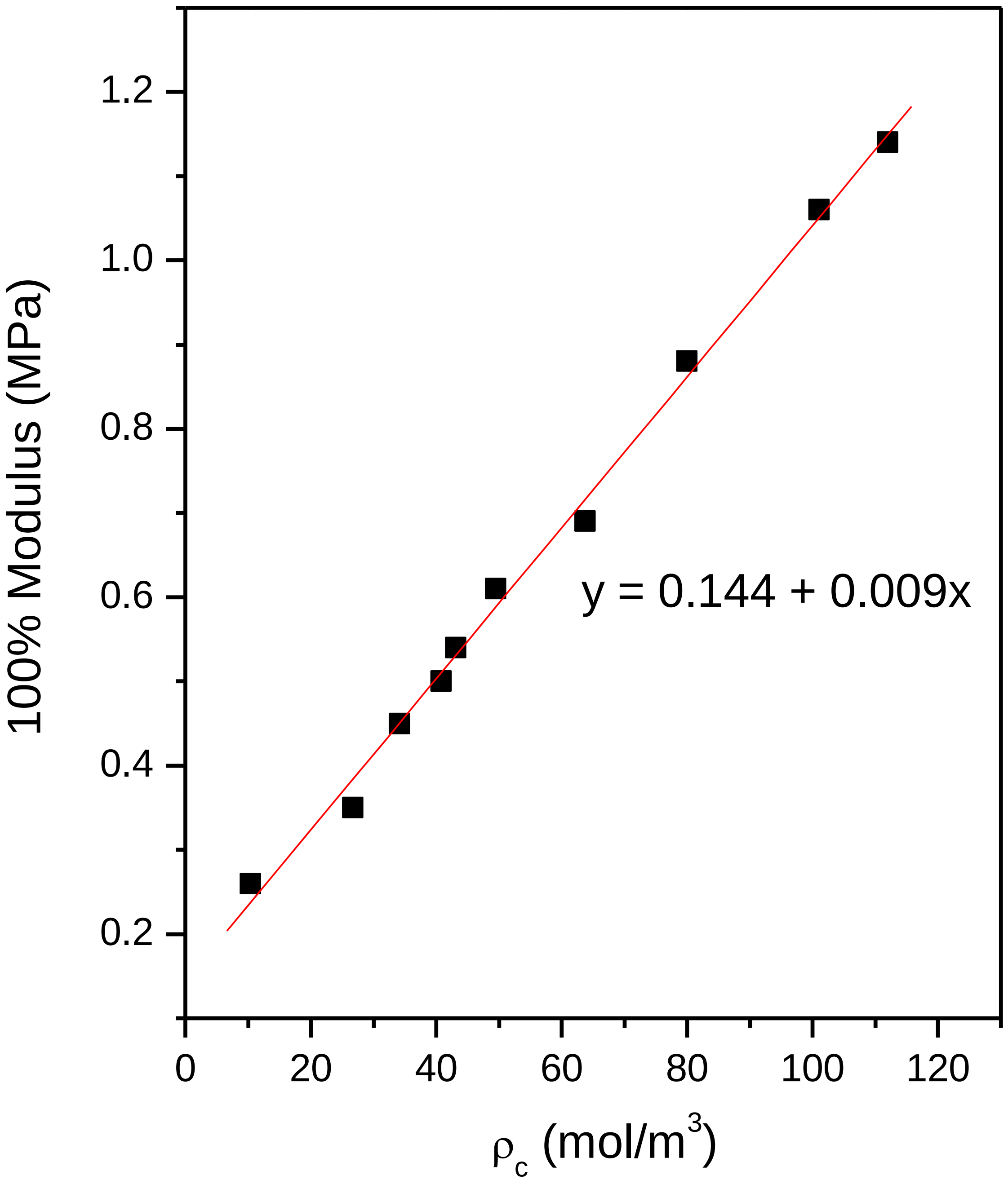

Figure 4. 9 100% modulus versus crosslink density of DCP cured gum NR vulcanizates.

4.4 Tear Test Results of DCP Cured Pre-cut Gum NR Vulcanizates

Log-log plots of tear strength versus cut size for all the DCP cured gum NR vulcanizates are shown in Figure 4.10 - Figure 4.19.

GD0.5 (Figure 4.10), the lightly crosslinked vulcanizate, its tear strength drops from the strong population (where bulk crystallization occurs prior to rupture) to the weak population (where lacks of bulk crystallization). There appears an unstable region in which strong population and weak population coexist. In this unstable region, even with the same cut size, some specimens may undergo bulk crystallization but others don't. Two critical cut sizes are used to define the width of the unstable region: the strong population critical cut size c_s and the weak population critical cut size c_w. Substantial bulk crystallization occurs in all the testpieces with cut size below c_s, before crack initiates thus resisting cut growth. And the testpieces with cut size above c_s are lack of bulk crystallization. In between, there is a possibility for bulk crystallization to take place. The average tensile strength σ_{b0} for the uncut specimens of GD0.5, marked as the solid line in Figure 4.10, overlaps or even is lower than the tear strength of specimens with small cut. An explanation for this phenomenon is the inevitable edge flaws contained in the normal tensile testpieces due to the cutting action of the die used to "click" them out, although no intentional pre-cut was made. Other factors like molding imperfections, dirt particles and inhomogeneity in vulcanizate structure also can results in inherent flaws[45]. Similar phenomenon also can be observed in other vulcanizates (GD1.0 – GD2.5).

For the moderately crosslinked vulcanizates, from GD1.0 to GD4.0 (Figure 4.11 – 4.17), behavior similar to GD0.5 can be observed. But the difference is that in their unstable regions, strengths distribute randomly and it's hard to tell the strong and weak populations. In this region, some specimens undergo crystallization but not bulkily. Differences in level of crystallinity for the testpieces result in the instability of strength in the unstable region. Compared with the lightly crosslinked GD0.5, their breaking strain just below c_s is smaller, which means substantial bulk crystallization occurs at higher strain for lightly crosslinked vulcanizates (800%) than moderately crosslinked vulcanizates (430% ~ 693%). It is apparent that crosslink density affects crystallizability. Flory[46] stated that crystallization begins at a lower strain for vulcanizates with higher crosslink density due to greater alignment of chains. As one of the moderately crosslinked vulcanizates, GD5.0 (Figure 4.18) show a different phenomenon. No unstable region could be observed in this vulcanizate. Strength drops abruptly from the strong population to weak population at a critical cut size c_{cr} ($c_{cr} = 0.12$mm).

No drop in strength can be found in the highly crosslinked vulcanizate GD6.0 (Figure 4.19). Strength decreases monotonically with the increase of cut size. According to the X-ray measurement results[47], crystallites initiate at about 250% strain for gum NR. The highest extension of GD 6.0 ($c \approx 0.11$ mm) is only 166%, which indicates that highly crosslinked vulcanizates do not crystalize and therefore have a low strength.

Figure 4.20 merges the tear test results of GD1.0 – GD4.0 together. Obviously, these vulcanizates have similar strength in the strong population and weak population. The vulcanizates with larger c_s have a larger strong population, which means they can keep better tear resistance at larger cut size compared with those with smaller c_s. It can be obviously seen that GD4.0 (in star shape) has a small c_s value (0.26 mm), so it may not endure fracture even the crack is small.

Trend lines for c_s, c_w and the width of unstable region Δc ($\Delta c = c_w - c_s$) as a function of crosslink density are plotted in Figure 4.21 and Figure 4.22. They show similar dependence on crosslink density: they all pass through a maximum at GD1.8 with the increase of crosslink density. Therefore, among all the vulcanizates, GD1.8 has the best tear resistance.

Figure 4.23 shows the tear test results of the majority of DCP cured gum NR vulcanizates (GD0.5, GD3.0, GD5.0 and GD6.0). Least squares lines are drawn for GD5.0 and GD6.0. GD0.5, as the lightly crosslinked vulcanizate, is weak but endure a relatively larger cut size than GD5.0. GD3.0 represents the moderately crosslinked vulcanizates GD1.0 – GD4.0, because they have the similar behavior. They are the strongest at all cut sizes. GD5.0 seems to be the critical one from the moderately crosslinked vulcanizates to highly crosslinked vulcanizates. It could be as strong as GD1.0 – GD4.0 when the cut size is smaller than the critical cut size and becomes as weak as the highly crosslinked GD6.0 when the cut size becomes larger. The highly crosslinked GD6.0 is the weakest because it does not crystallize at all cut sizes. Unstable region can only be observed in lightly and most of the moderately crosslinked vulcanizates. Like the uncut specimens, tear strength of DCP cured gum NR vulcanizates passes through a maximum at the moderately crosslinked vulcanizates as a function of crosslink density.

Crack paths for precut specimens of all the DCP cured gum NR vulcanizates were simple. In all cases, direct propagation occurred across the specimens. Crack surfaces were smooth and no secondary cracking was observed. Crack path is almost 90° to the loading direction.

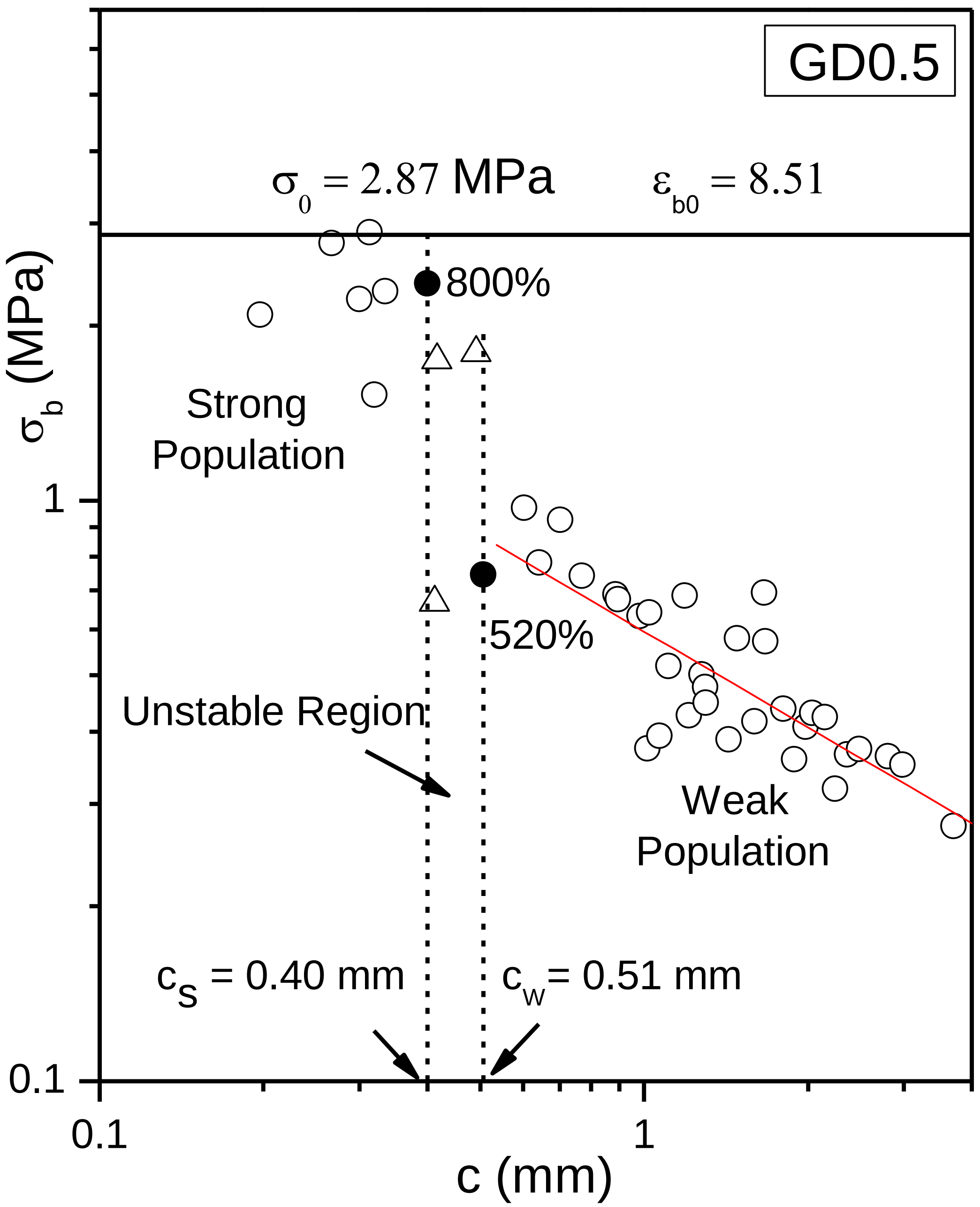

Figure 4. 10 Tear strength versus cut size of GD0.5. Horizontal solid line denotes normal tensile strength for GD0.5. Vertical dotted lines show the values of cs and cw, beside which the numbers in percentage are the breaking strains for the specimens with critical cut seizes plotted in solid circles. Strong population, weak population and unstable region are marked in this figure.

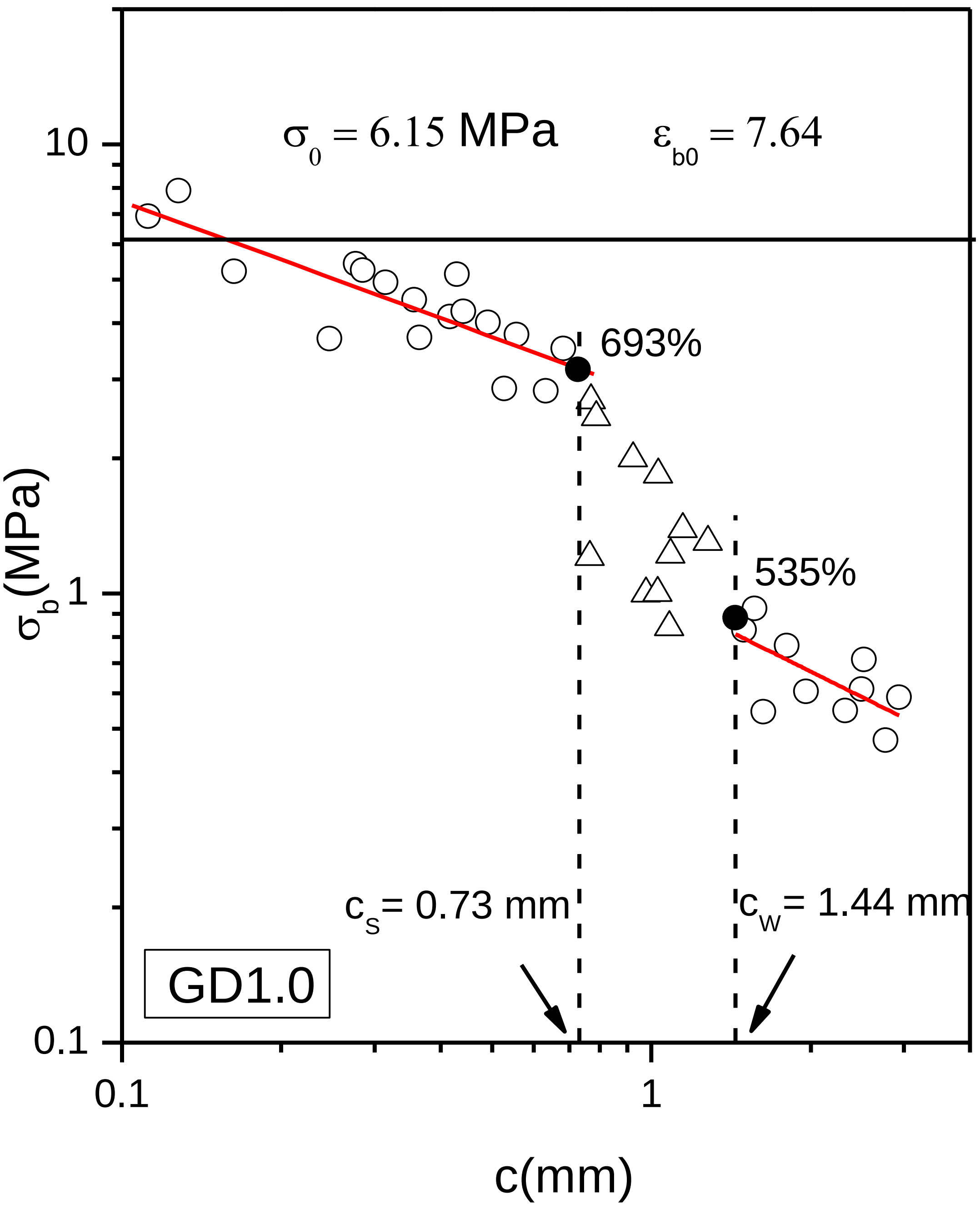

Figure 4. 11 Tear strength versus cut size of GD1.0. Horizontal solid line denotes normal tensile strength for GD1.0. Vertical dotted lines show the values of cs and cw, beside which the numbers in percentage are the breaking strains for the specimens with critical cut seizes plotted in solid circles.

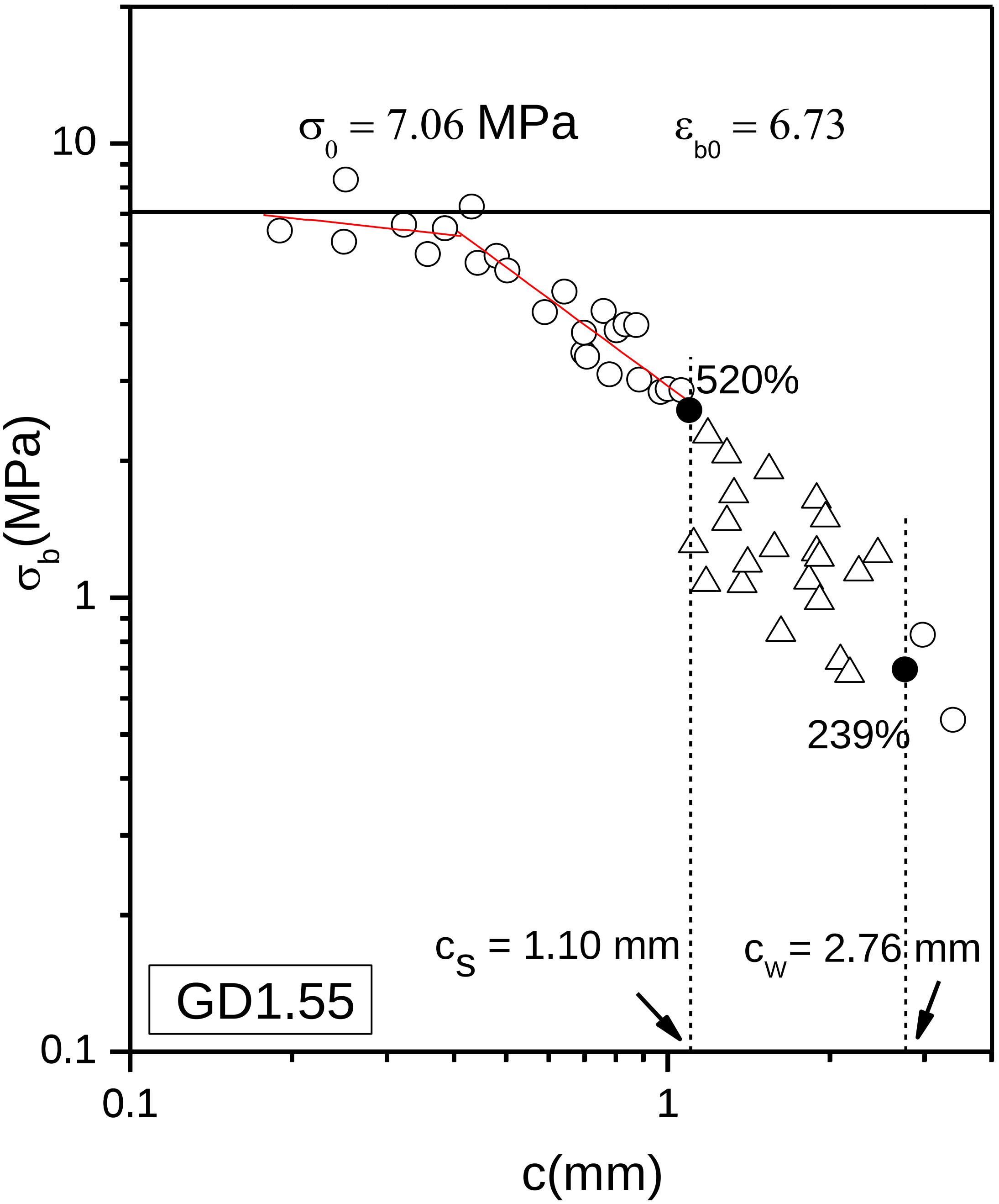

Figure 4. 12 Tear strength versus cut size of GD1.55. Horizontal solid line denotes normal tensile strength for GD1.55. Vertical dotted lines show the values of cs and cw, beside which the numbers in percentage are the breaking strains for the specimens with critical cut seizes plotted in solid circles.

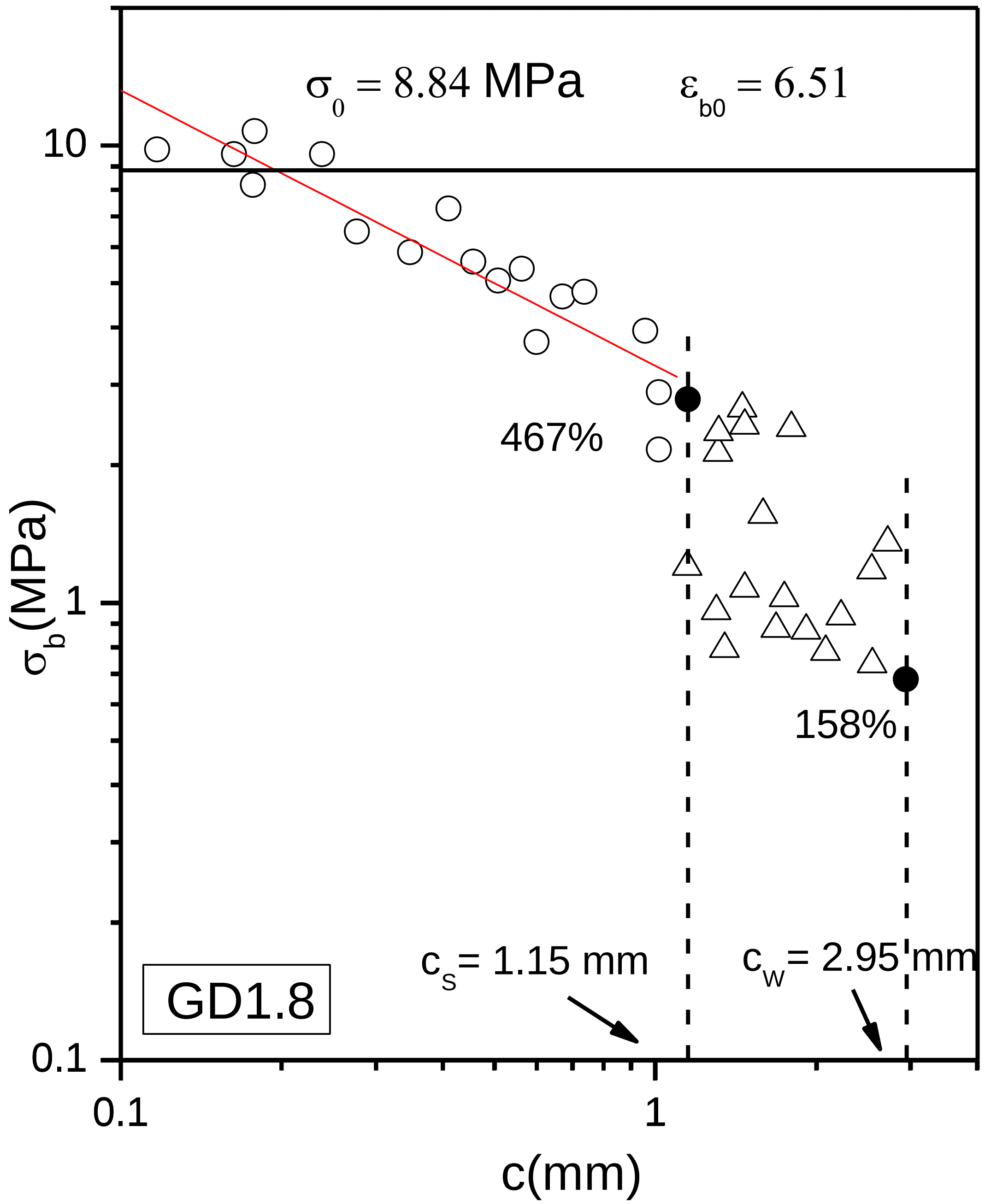

Figure 4. 13 Tear strength versus cut size of GD1.8. Horizontal solid line denotes normal tensile strength for GD1.8. Vertical dotted lines show the values of cs and cw, beside which the numbers in percentage are the breaking strains for the specimens with critical cut seizes plotted in solid circles.

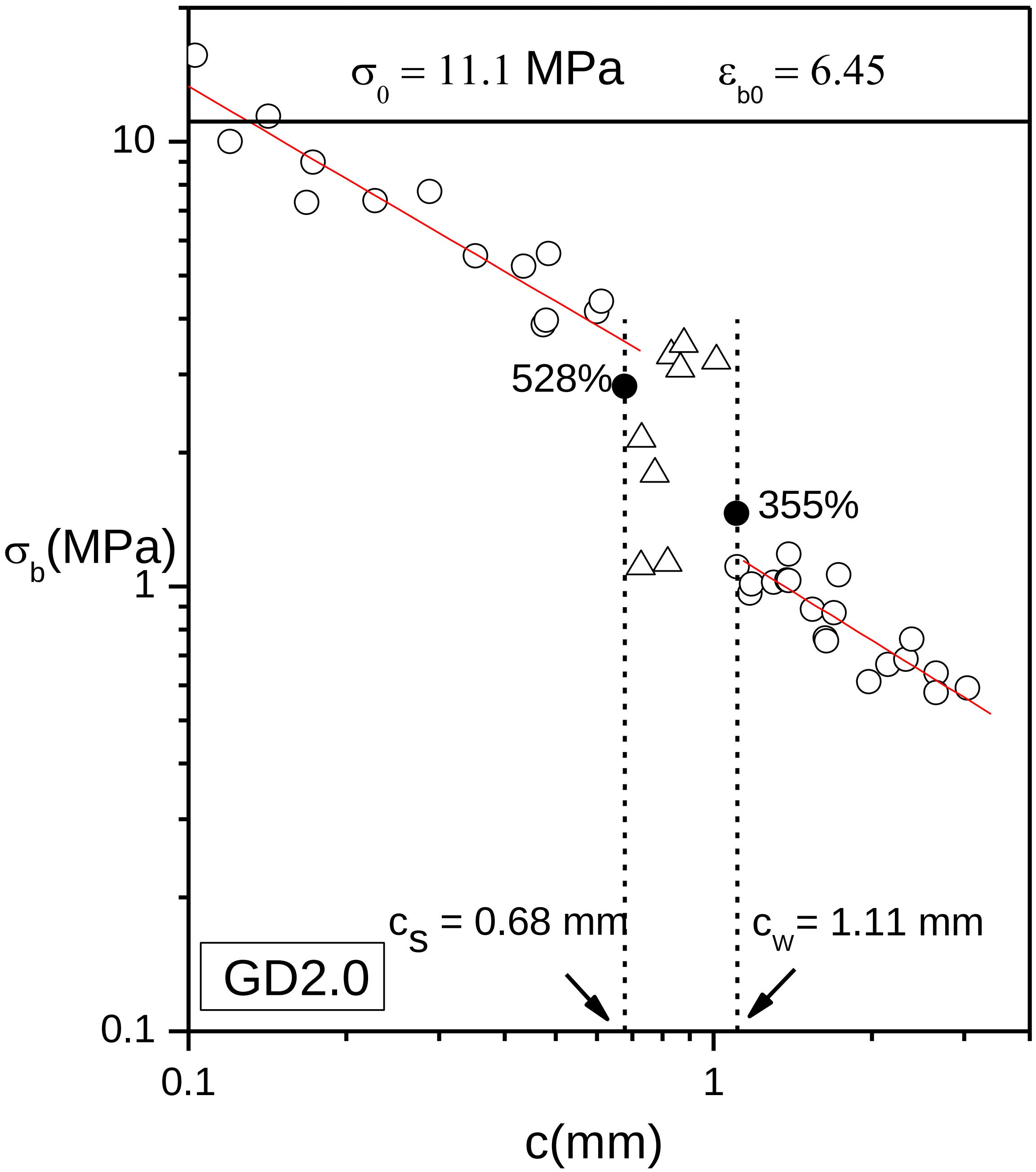

Figure 4. 14 Tear strength versus cut size of GD2.0. Horizontal solid line denotes normal tensile strength for GD2.0. Vertical dotted lines show the values of cs and cw, beside which the numbers in percentage are the breaking strains for the specimens with critical cut seizes plotted in solid circles.

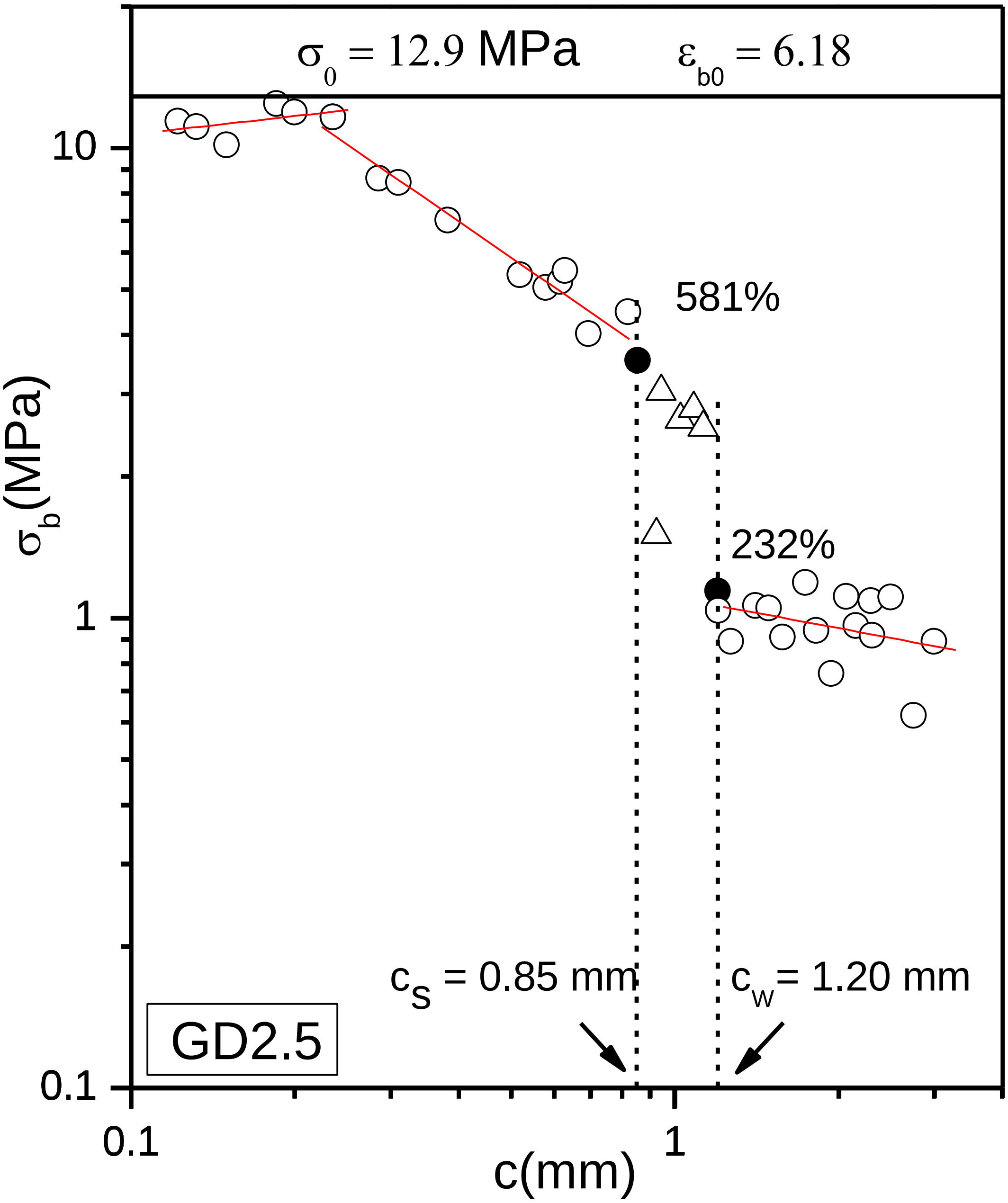

Figure 4. 15 Tear strength versus cut size of GD2.5. Horizontal solid line denotes normal tensile strength for GD2.5. Vertical dotted lines show the values of cs and cw, beside which the numbers in percentage are the breaking strains for the specimens with critical cut seizes plotted in solid circles.

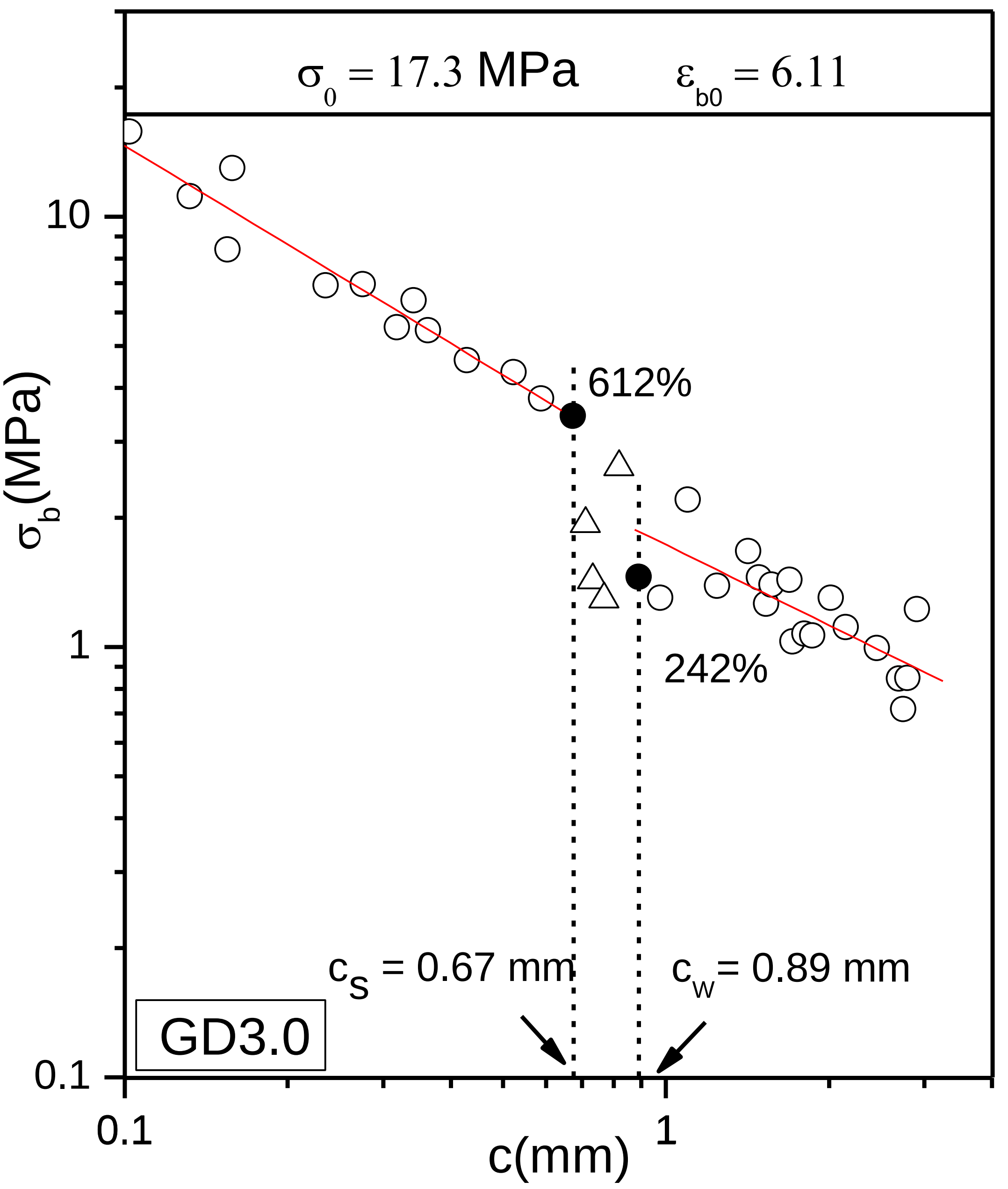

Figure 4. 16 Tear strength versus cut size of GD3.0. Horizontal solid line denotes normal tensile strength for GD3.0. Vertical dotted lines show the values of cs and cw, beside which the numbers in percentage are the breaking strains for the specimens with critical cut seizes plotted in solid circles.

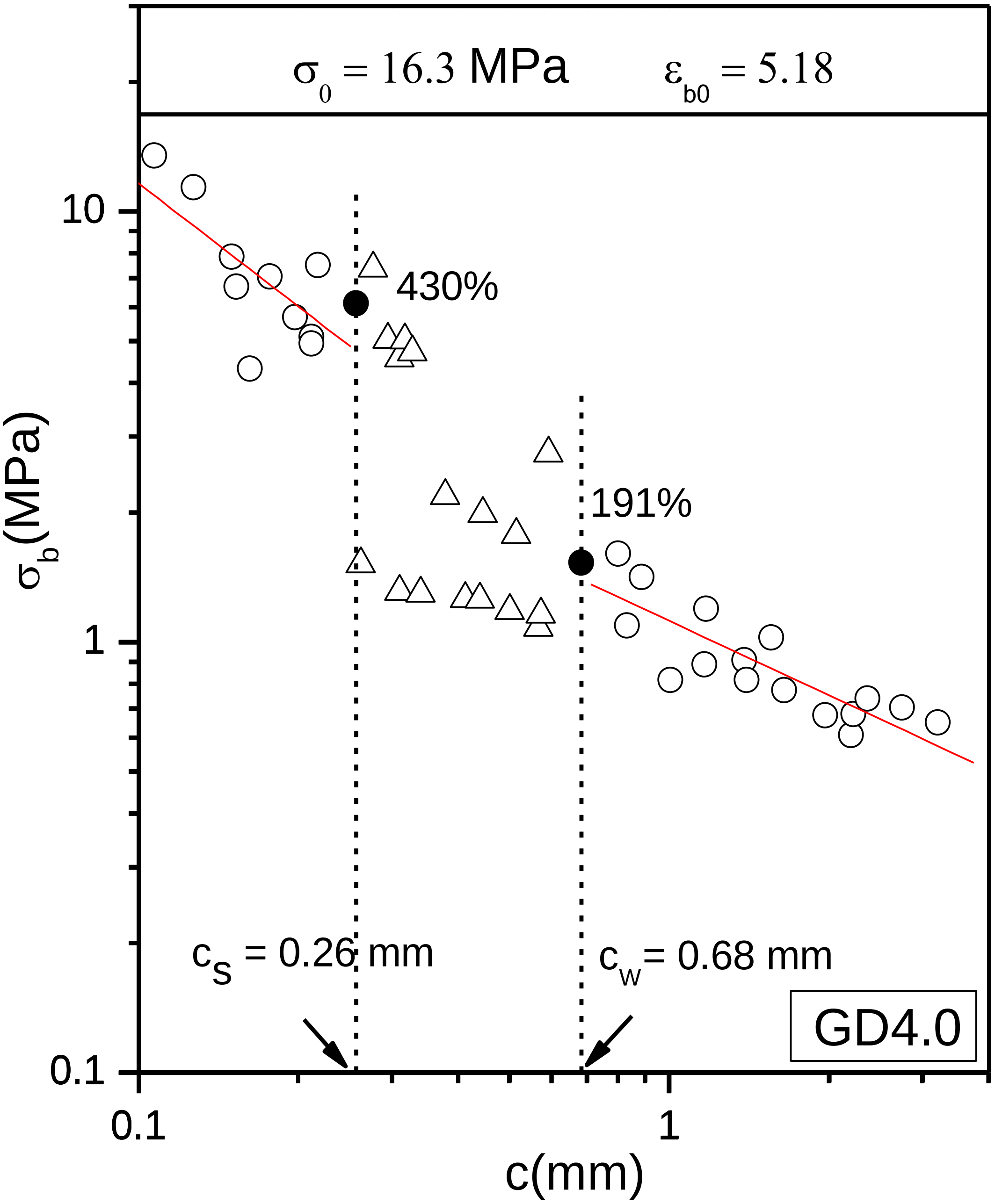

Figure 4. 17 Tear strength versus cut size of GD4.0. Horizontal solid line denotes normal tensile strength for GD4.0. Vertical dotted lines show the values of cs and cw, beside which the numbers in percentage are the breaking strains for the specimens with critical cut seizes plotted in solid circles.

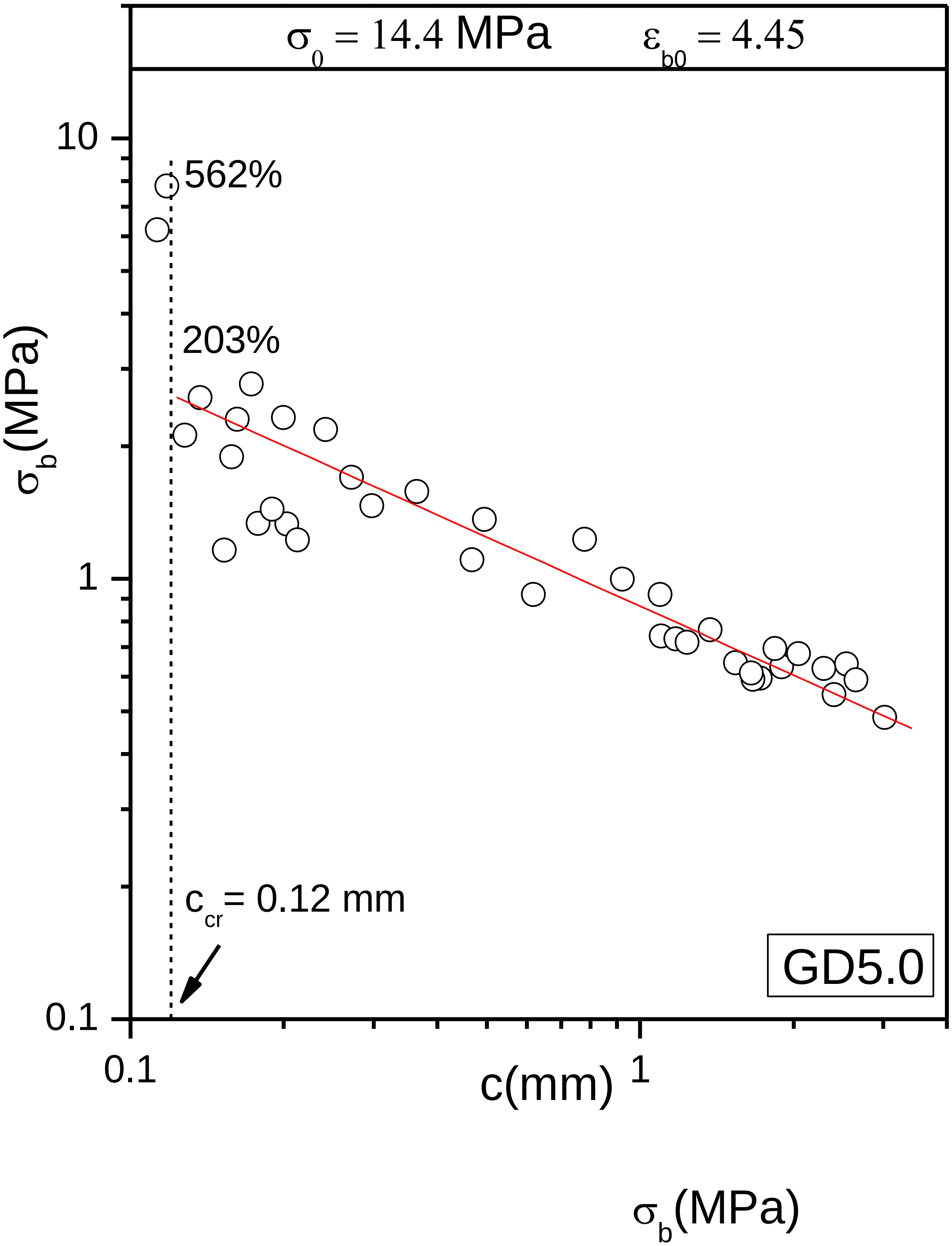

Figure 4. 18 Tear strength versus cut size of GD5.0. Horizontal solid line denotes normal tensile strength for GD5.0. Vertical dotted lines show the values of cs and cw, beside which the numbers in percentage are the breaking strains for the specimens with critical cut seizes plotted in solid circles.

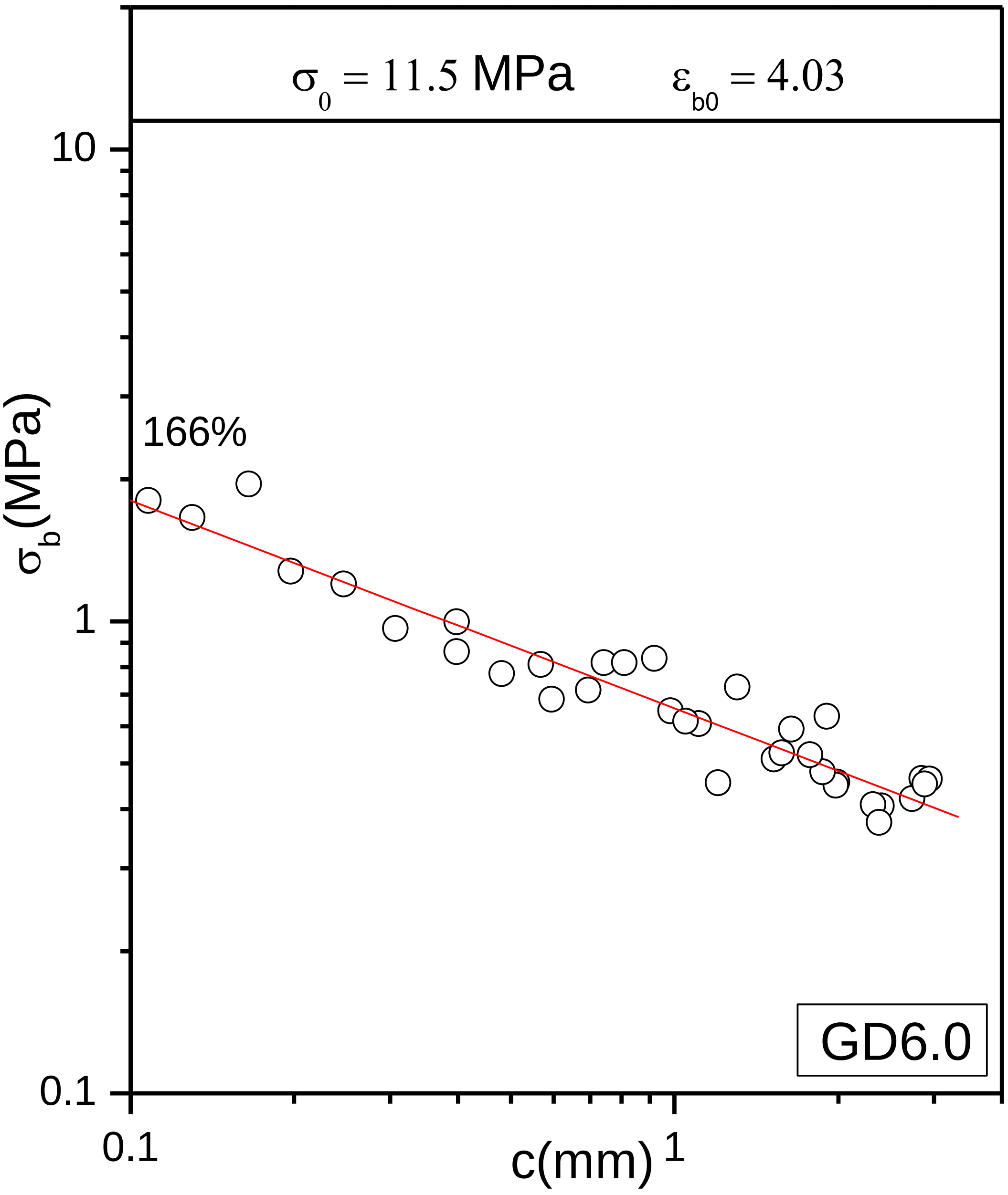

Figure 4. 19 Tear strength versus cut size of GD6.0. Horizontal solid line denotes normal tensile strength for GD6.0. Vertical dotted lines show the values of cs and cw, beside which the numbers in percentage are the breaking strains for the specimens with critical cut seizes plotted in solid circles.

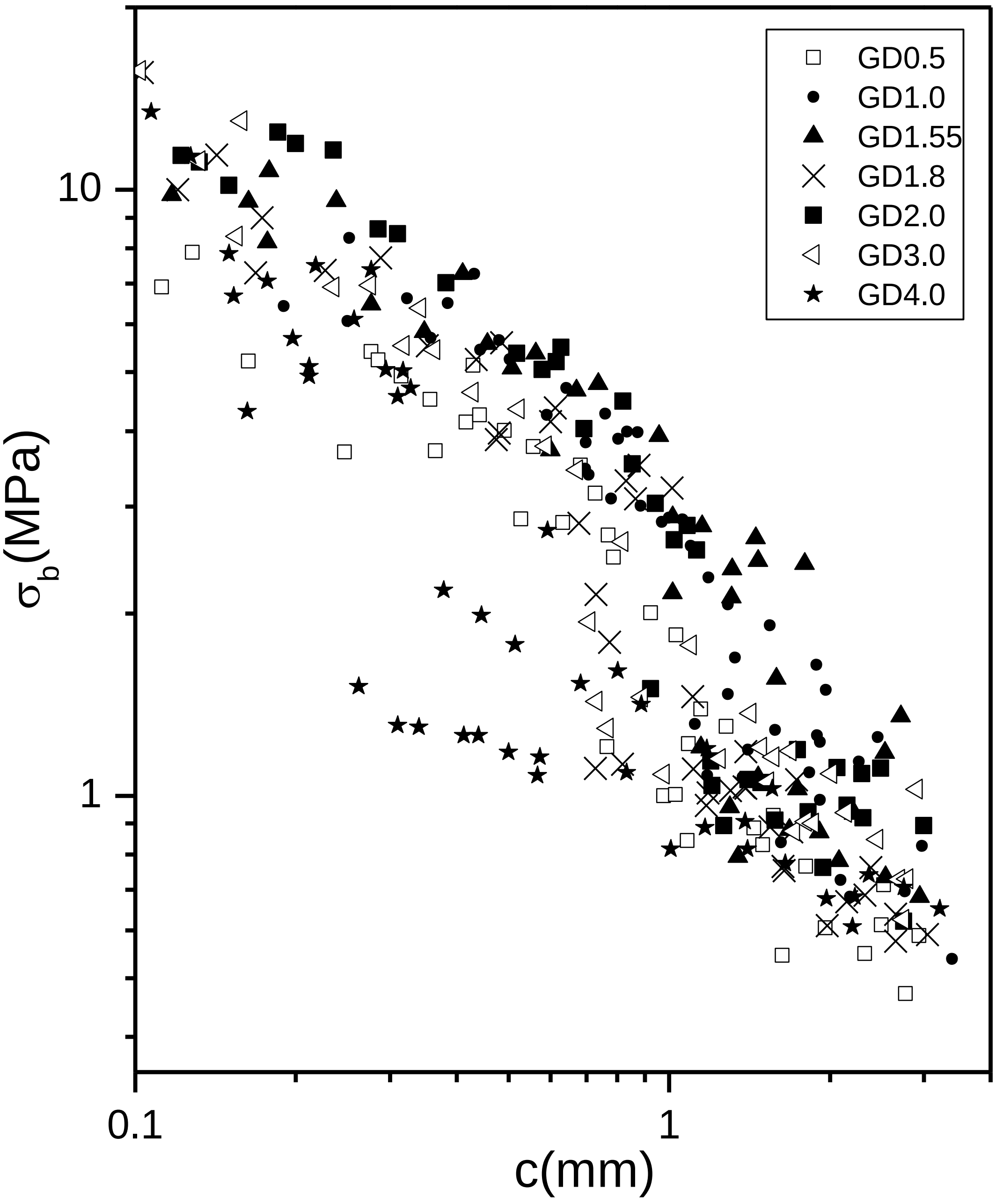

Figure 4. 20 Tear strength versus cut size of moderately crosslinked vulcanizates (GD1.0 – GD4.0).

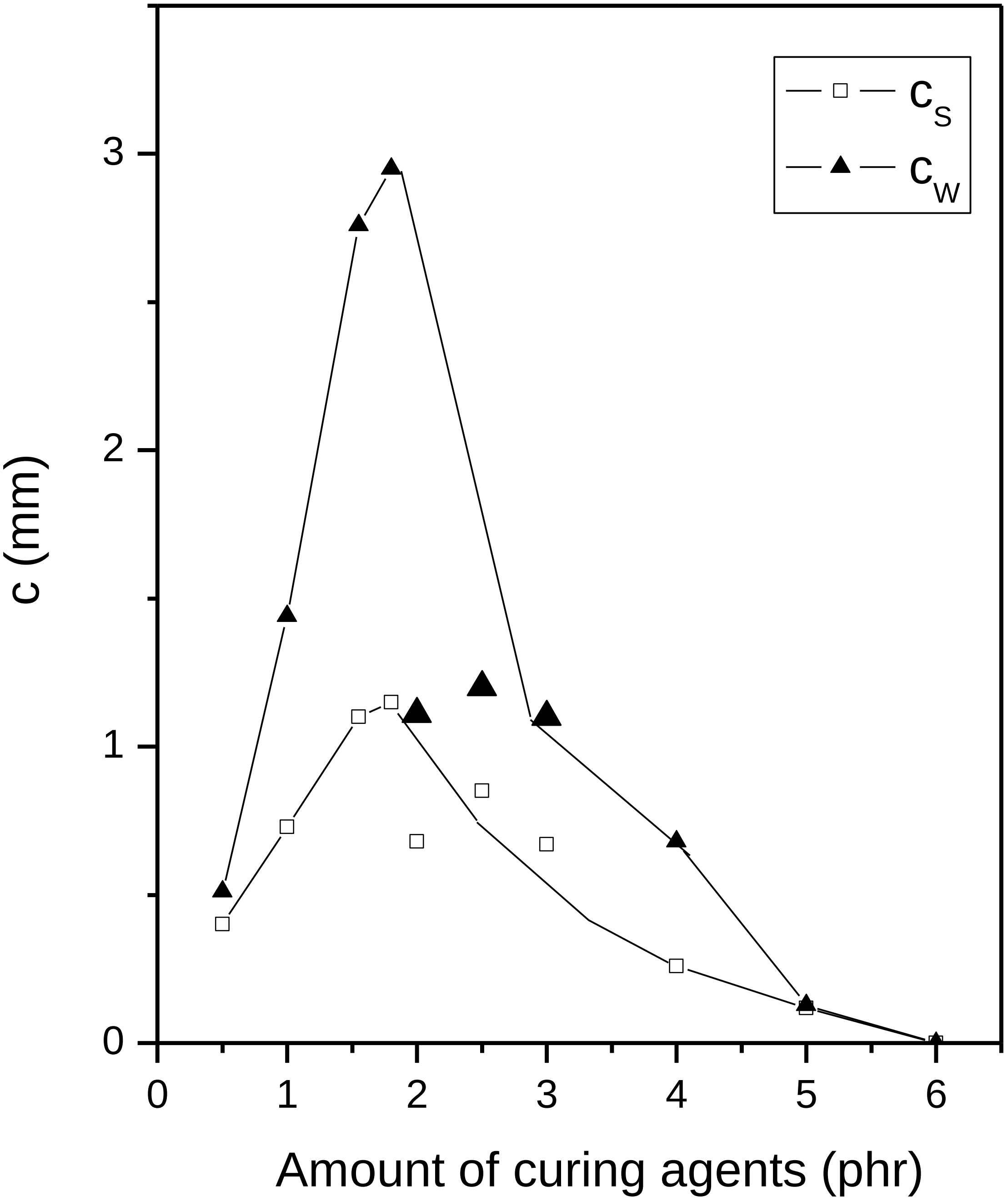

Figure 4. 21 Trend lines for cs and c_w.

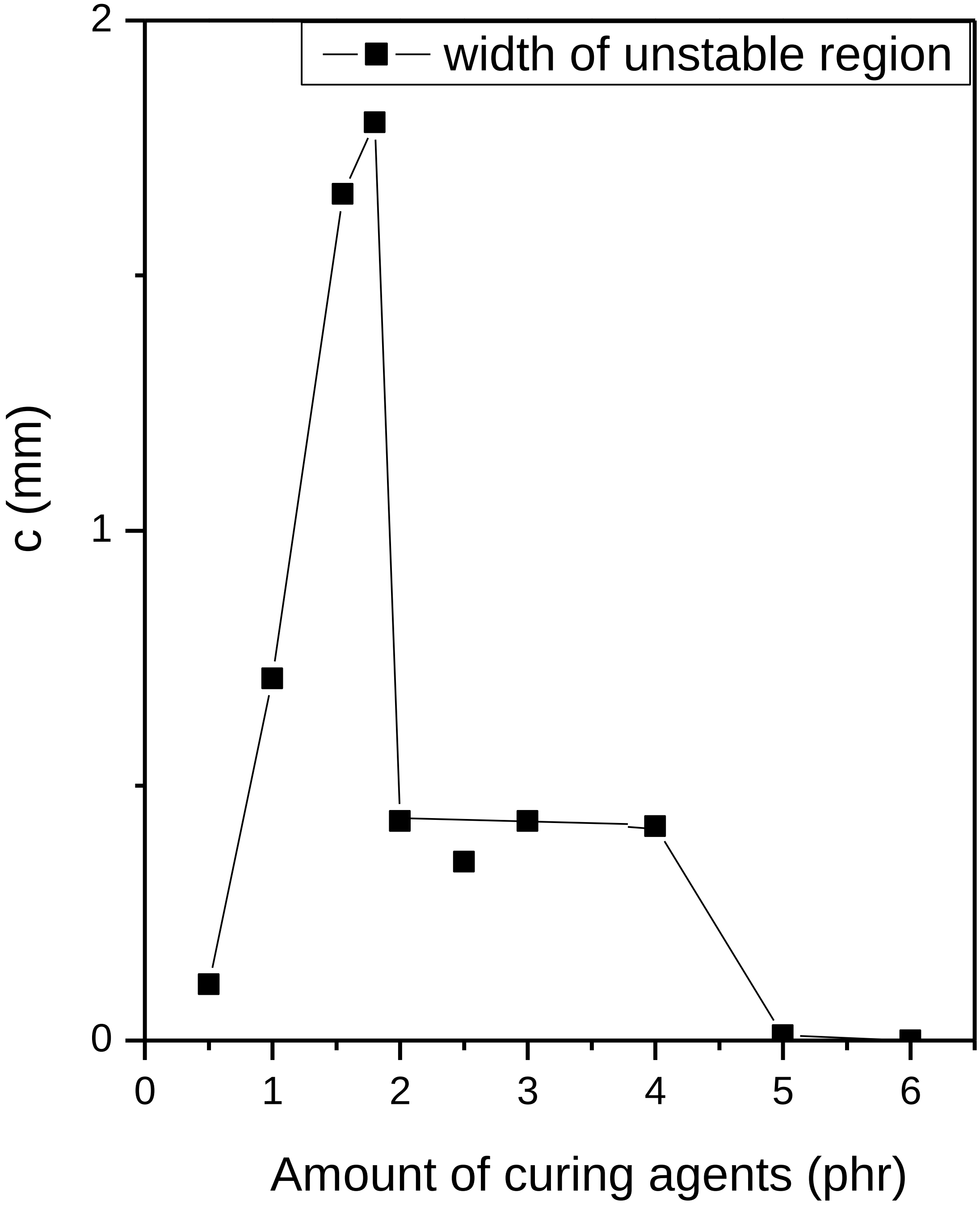

Figure 4. 22 Trend lines for Δ*c*.

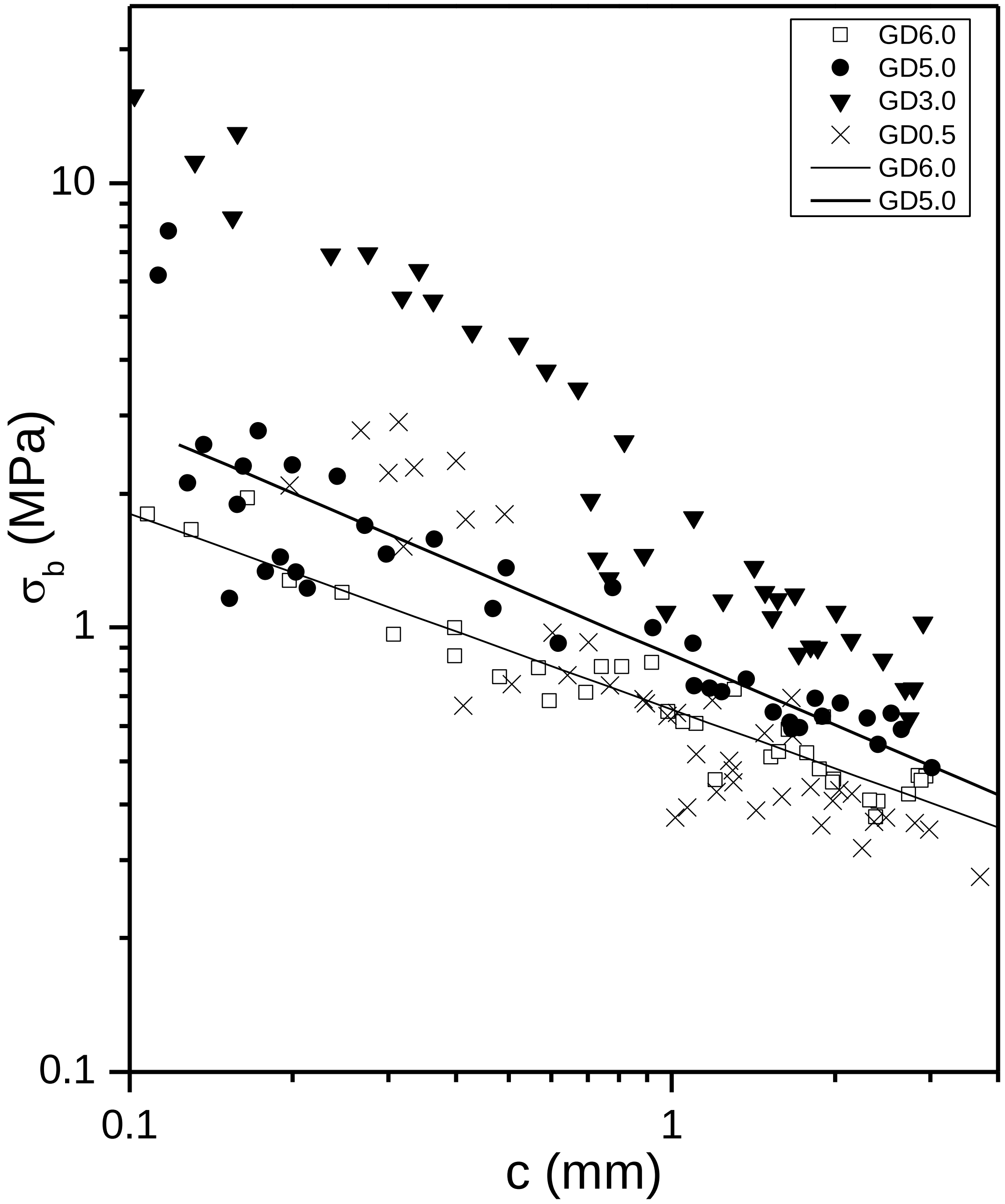

Figure 4. 23 Tear strength versus cut size of the majority of DCP cured gum NR vulcanizates (GD0.5, GD3.0, GD5.0 and GD6.0).

4.5 Comparison of the Properties of Sulfur and DCP Cured Gum NR Vulcanizates

4.5.1 Comparison of Normal Tensile Test Results

Figure 4.24, 4.25 and 4.26 compare the normal tensile test results of DCP and sulfur cured gum NR vulcanizates. Normal tensile strength σ_{b0}, ultimate elongation ε_{b0} and 100% modulus of S & DCP cured gum NR show the similar dependence on crosslink density ρ_c.

The normal tensile strength of both DCP and sulfur cured gum NR pass through a maximum with the increase of crosslink density (Figure 4.24). Sulfur cured gum NR has much larger σ_{b0} values. The difference is quite large at the crosslink density around 75 – 100 mol/m^3, where strength starts to go a downward trend for DCP cured gum NR while the sulfur one is still at a maximum value. This is due to a better energy dissipation mechanism of sulfur cured gum NR which can be explained by the flexibility of the sulfur bonds. When the number of crosslinks passes the optimum value, chains are restricted, so fewer energy could be dissipated and brittle fracture starts. But sulfur bonds are more flexible and they could reform after broken so the sulfur cured gum NR can reach a larger strength before fracture.

The ultimate elongation decreases monotonically with crosslink density (Figure 4.25). Polysulfide crosslinks are more flexible than the carbon-carbon bonds crosslinks, so they have better extensibility and don’t break immediately like the carbon-carbon bonds. That’s the results for larger ultimate elongation of sulfur cured gum NR. However, according to the least squares fitting lines, the ultimate elongation of DCP and sulfur cured gum rubber will be similar when the crosslink is large, which means the flexibility of sulfur bonds don’t work with the tightly crosslinked structure.

100% modulus increases linearly with increasing crosslink density (Figure 4.26). 100% modulus of DCP and sulfur cured gum NR are similar. The rubbery tensile modulus is dependent on the crosslink density, but nearly independent of the crosslink type[48].

4.5.2 Comparison of Tear Test Results

Tear strengths as a function of cut size of UA1.0x and GD3.0 are compared in Figure 4.27. A designation of UA1.0x means an unfilled sulfur cured NR contains antioxidant and the reference level is 1.0 times of curatives[40]. GD3.0 is the gum NR cured with 3.0 phr DCP. UA1.0x and GD3.0 have similar crosslink densities ($\rho_c \approx 64$ mol/m^3). A 10 MPa difference in normal tensile strength of UA1.0x and GD3.0 is illustrated by the solid lines. Only two populations can be observed in UA1.0x, strong population and weak population, while, except these two populations, an unstable region appears in GD3.0. Bulk crystallization starts at lower strain for sulfur cured gum NR than DCP cured gum NR. The polysulfide crosslinking bonds are more flexible so that they align faster and thus initiate bulk crystallization at lower strain (492%). On the contrary, the carbon-carbon bonds needs more time to move and align, which makes DCP cured gum NR bulky crystallize at a larger strain. UA1.0x has larger tear strength in the strong population than GD3.0, which can be explained similarly as discussed in 4.5.1, a better energy dissipation mechanism of sulfur cured gum NR. However, it's interesting that they show similar tear strength in the weak population. At large cut, stress concentration is large and there is no time for crystallization to take place, neither for sulfur bonds to reform. Crack quickly goes through the specimen and specimen fractures.

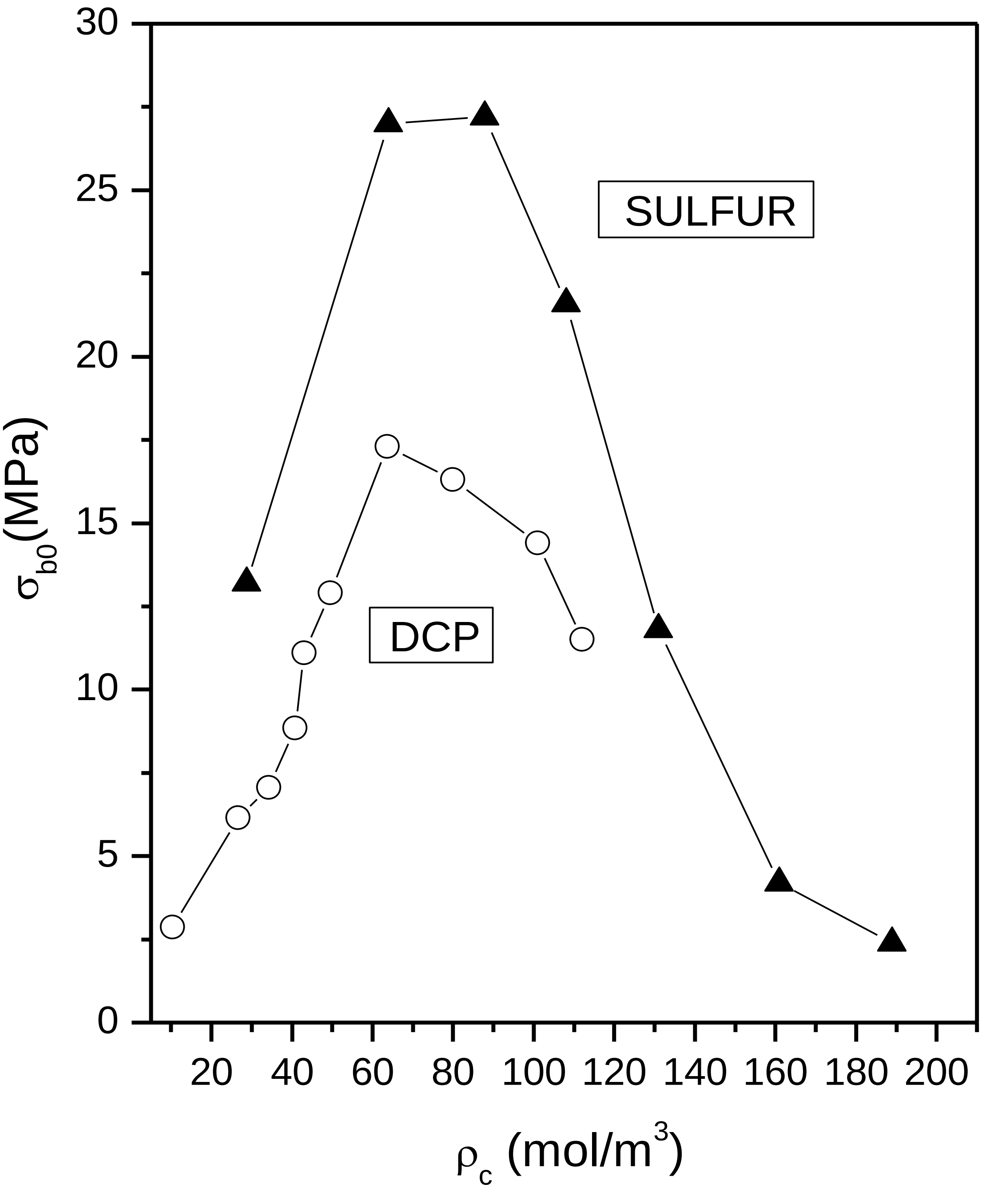

Figure 4. 24 Effect of crosslink density on normal tensile strength b0 of DCP and Sulfur cured gum NR vulcanizates.

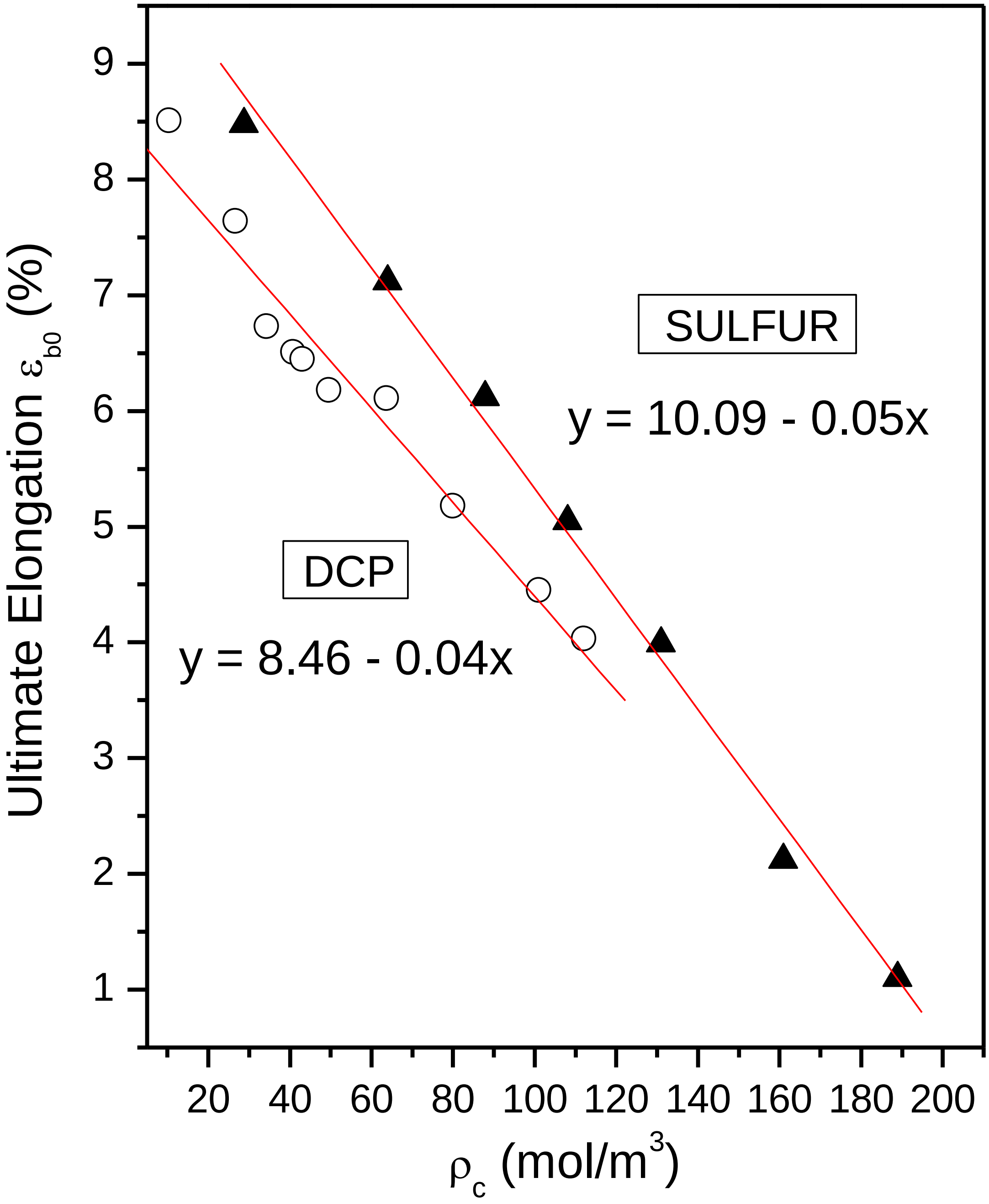

Figure 4. 25 Effect of crosslink density on ultimate elongation b0 of DCP and Sulfur cured gum NR vulcanizates.

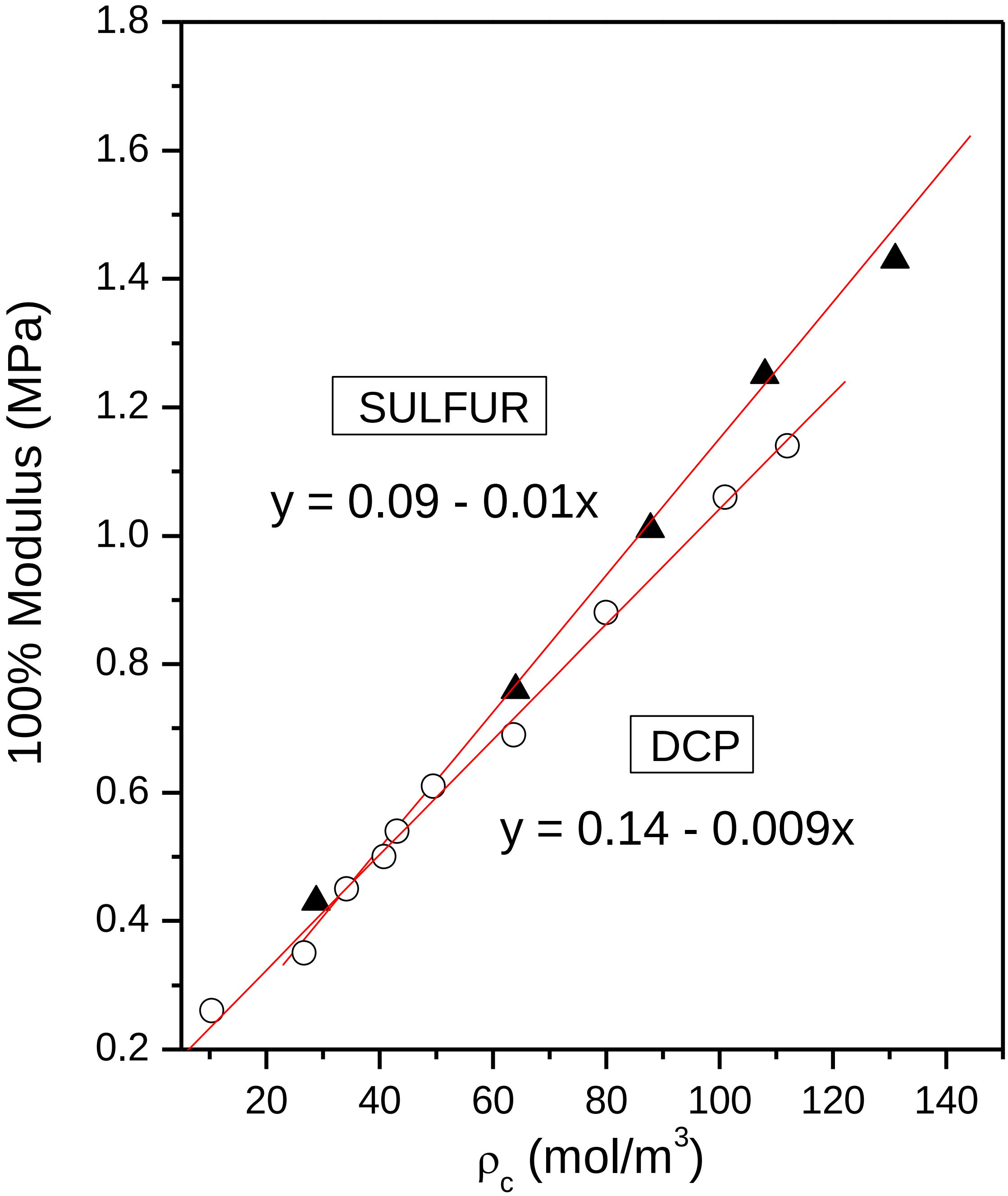

Figure 4. 26 Effect of crosslink density on 100% modulus of DCP and Sulfur cured gum NR vulcanizates.

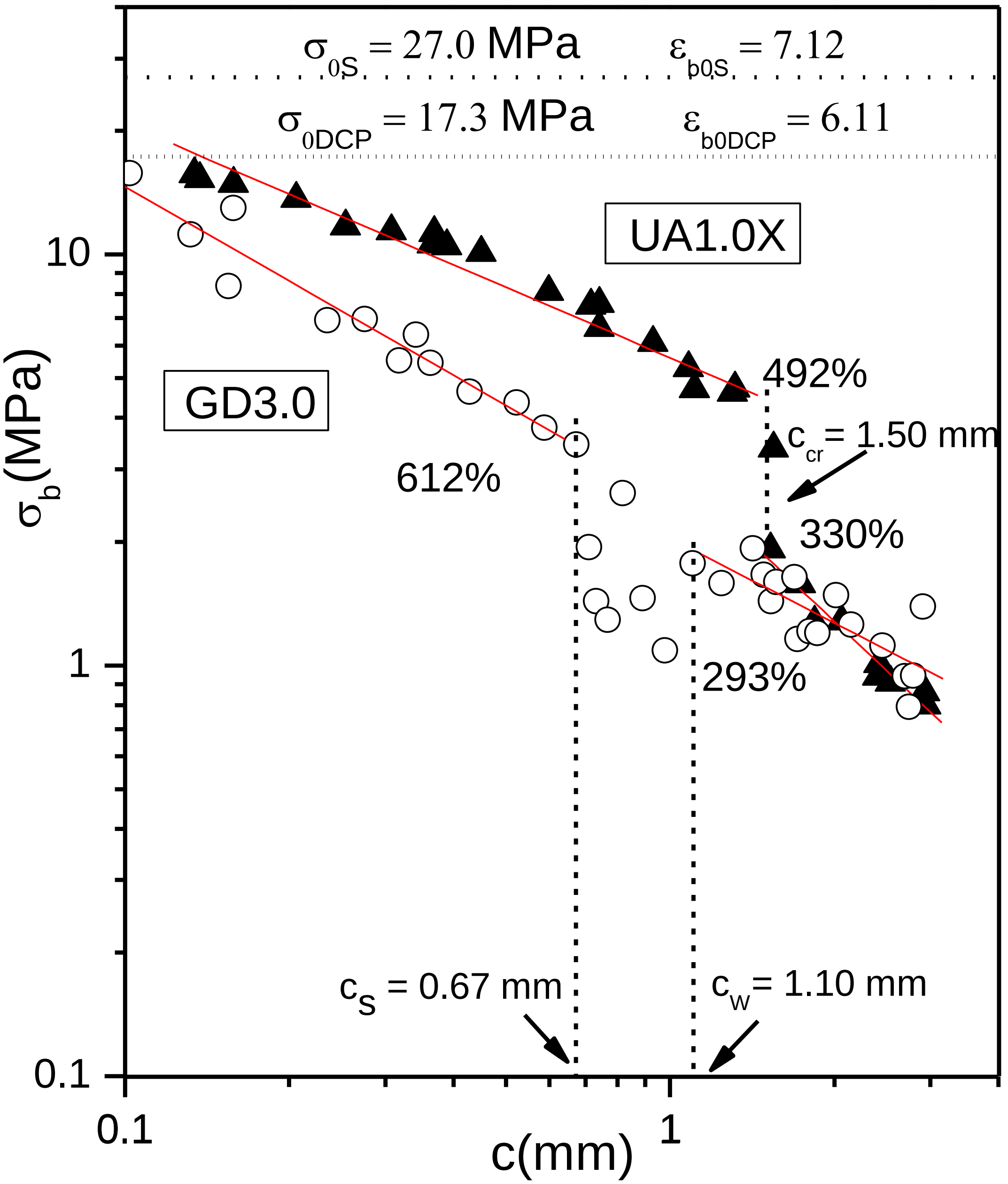

Figure 4. 27 Effect of cut size on tear strength of DCP and Sulfur cured gum NR vulcanizates with similar crosslink density. Horizontal solid line denotes normal tensile strength. Vertical dotted lines show the values of c_s, c_w and c_{cr}, beside which the numbers in percentage are the breaking strains for the specimens with critical cut seizes.

CHAPTER VI

CONCLUSION

1. Normal tensile strength, ultimate elongation and 100% modulus of sulfur and DCP cured gum NR show similar dependence on crosslink density.

2. Normal tensile properties of sulfur and DCP cured gum NR decrease after crosslink density reaches an optimum. Sulfur cured gum NR has better strength than DCP cured gum NR.

3. The rubbery tensile modulus is dependent on the crosslink density, but nearly independent of the crosslink type.

4. For both sulfur and DCP cured gum NR, Lightly and moderately crosslinked samples show a slope change in tear strength, while tear strength of highly crosslinked samples decrease continuously with the increase of cut size. With an increase of crosslink density, tear resistance becomes worse, more brittle.

5. An unstable region is only observed in DCP cured gum NR, in which tear strength does not drop abruptly as the sulfur cured system.

6. With similar crosslink density, sulfur cured gum NR has a stronger tear strength at small cut size, whereas tear strength is similar for both sulfur and DCP cured gum NR when cut size is large enough.

7. For sulfur and DCP cured gum NR, strength and critical cut size, both properties indicative of strain crystallization, were maximized at moderate crosslink density. At

high crosslink density, no critical cut size was seen and samples were weak for all values of cut sizes, like gum SBR (amorphous rubber). The highly crosslinked gum NR samples, even if not precut, do not strain-crystallize prior to fracture.

REFERENCES

1. Hofmann, W. Natural Rubber. *Rubber Technology Handbook*; Hanser Publisher: New York, 1988.

2. Morton, M. Natural Rubber. *Rubber Technology*, 3rd ed.; Van Nostrand Reinhold: New York, 1987.

3. Woods, L.A. Crystallization Phenomena in Natural and Synthetic Rubbers. Advances in Colloid Science; American Chemical Society: New York, 1946; vol. 2.

4. Loan, L. D. Mechanism of Peroxide Vulcanization of Elastomers. Rubber Chem. Technol. 1967, 40, 149.

5. Dluzneski, P. R. Peroxide Vulcanization of Elastomers. Rubber Chem. Technol. 2001, 74.

6. Kmiec, C.; Kamath, V. Rubber world.1983, 189, 26.

7. Sheppard, C.; Kamath, V. Polym. Eng. Sci.1979, 19, 597.

8. Vroomen, G. L. M.; Visser, G. W. Rubber world. **1991**, *205*, 23.

9. Weast, R. C. CRC Handbook of Chemistry and Physics, CRC Press: Boca Raton, 1988.

10. Zhou, W.; Zhu, S. Macromolecules. 1998, 31, 435.

11. Loan, L. D. J. Appl. Polym. Sci. 1963, 7, 2259.

12. Gonzalez, L.; Rodriguez, A.; Marcos-Fernandez, A. Recent Res. Dev. Polym. Sci. 1998, 2, 485.

13. Kirchgessner, R. K.; Kamath, V. R.; Sheppard, C. S. Stromberg, S. E. Mod. Plast. 1984, 66.

14. Loan, L. D. Rubber Chem. Technol. 1967, 40, 149.

15. Yu, Q.; Zhu, S. Polymer. 1999, 40, 2961.

16. Class, J. Rubber World. 1999, 220, 35.

17. Ogunniyi, D. Prog. Rubber Plast. Technol. 1999, 15, 95.

18. Tuccio, A. Rubber World. 1994, 209, 34.

19. Lazar, M.; Hrckova, L.; Borsig, E.; Marcincin, A.; Reichelt, N.; Ratzch, M.; J. Appl. Polym. Sci. 2000, 78, 886.

20. Braun, D.; Richter, S.; Hellman, P, G.; Ratzsch, M. J. Appl. Polym. Sci. 2000, 78, 886.

21. Yu, Q.; Zhu, S.; Zhou, W. J. Polym. Sci., Part A: Poly,. Chem. 1998, 36, 851.

22. Busci, A.; Szocs, F.; Macromol. Chem. Phys. 2000, 201, 435.

23. Gilbert, M.; Garcia-Quesada, J. Plast. Rubber and Compos. 1999, 28, 125.

24. Coran, A. Y. Vulcanization Science and Technology of Rubber, J. E. Mark, Erman and F. R. Eirich, Eds., Elsevier Academic Press: San Diego, 2005.

25. RLHUDSON wibesite. http://www.rlhudson.com/O-Ring%20Book/selecting-batch.html. [Accessed 9 April, 2012].

26. Gonzalez, L.; Rodriguez, A.; Marcos, A.; Chamorro, C. Kautsch. Gummi Kunstst. 1998, 51, 83.

27. Stern, H. J. Rubber: Natural and Synthetic, Maclaren and Sons Ltd.: London, 1967.

28. Thomas, D. K. Crosslinking Efficiency of Dicumyl Peroxide in Natural Rubber. 1962, VI, 613.

29. Flory, P. J. Principles of Polymer Chemistry, Cornell University Press: Ithac, N.Y. 1953.

30. Treloar, L. R. G. The Physics of Rubber Elasticity, Clarendon Press: Oxford, 1975.

31. Mark, J. E. J. Chem. Educ. 1981, 58, 898.

32. Flory, P. J.; Rehner, J. Statistical Mechanics of Cross-Linked Polymer Networks I. Rubberlike Elasticity. J. Chem. Phys. 1943, 11, 512.

33. Flory, P. J.; Rehner, J. Statistical Mechanics of Cross-Linked Polymer Networks II. Swelling. J. Chem. Phys. 1943, 11, 521.

34. Rivlin, R. S. Saunders, D. W. Large Elastic Deformation of Isotropic Materials VII. Experiments on the Deformation of Rubber. Phil. Trans. Roy. Soc. 1951, A243, 25.

35. Inglis, C. E. Stresses in a Plate Due to the Presence of Cracks and Sharp Corners Trans.; Inst. Naval Architects: London, 1913.

36. Hamed, G. R. Energy Dissipation and the Fracture of Rubber Vulcanizates. Rubber Chem. Technol. 1991, 64, 493.

37. Gent, A. N. Strength of Elastomers. Science and Technology of Rubber Elsevier Academic Press, San Diego, 2005.

38. Hamed, G. R. Rubber Chem. Technol. 1994, 67, 531.

39. Thomas, A.G.; Whittle, J.M. Tensile Rupture of Rubber. Rubber Chem. Technol. 1970, 43, 222.

40. Hamed, G. R.; Rattanasom, N. Effect of Crosslink Density on Cut Growth in Gum Natural Rubber Vulcanizates. Rubber Chem. Technol. 2002, 75, 323.

41. Bristow, G. M.; Watson, W. F. Cohesive Energy Densities of Polymers. Trans. Faraday Soc. 1985, 54, 1734.

42. Deuri, A. S.; Bhowmick, A. K. Effect of Aging on Critical Cut Length and Morphology of Fracture Surface in Tensile Rupture of Natural Rubber. J. Mater. Sci. 1987, 22, 4299.

43. Lake, G. J., Thomas, A.G. The Strength of Highly Elastic Materials. Proc. R. Soc. (Lond). 1967, 300, 108–19.

44. Hamed, G. R. Fundamental Characteristics and Properties of Crosslinked Elastomers. Rubber World. 1994, 211, 25.

45. Hamed, G. R. Tearing of Vulcanized Rubber. Rubber Chem. Technol. 2005, 78, 550.

46. Flory, P. J. Effect of Molecular Structure on Physical Properties of Butyl Rubber. Ind. Eng. Chem. 1946, 38, 417.

47. Gehman, S. D., Field, J. E. X-Ray Structure of Rubber – Carbon Black Mixtures. Ind. Eng. Chem. 1940, 32, 1401.

48. Patterson, E., Backman, D., Cloud, G. Composite Materials and Joining Technologies for Composites, Volume 7. Springer: London, 2012.

APPENDIX

DATA FROM FIGURES AND RESULTS OF VARIOUS VULCANIZATES

A1: Tensile properties of GD0.5.

Specimen #	c (mm)	Thickness (mm)	σ_{bc} (MPa)	ε_{bc} (%)
1	0.20	0.520	2.09	815
2	0.27	0.548	2.77	779
3	0.30	0.425	2.22	749
4	0.31	0.518	2.90	837
5	0.32	0.507	1.52	655
6	0.34	0.515	2.29	762
7	0.40	0.545	2.37	800
8	0.41	0.519	0.67	447
9	0.42	0.545	1.75	730
10	0.49	0.548	1.80	(45)
11	0.51	0.547	0.75	520
12	0.60	0.446	0.97	887
13	0.64	0.535	0.78	507
14	0.70	0.569	0.93	576
15	0.77	0.557	0.74	445
16	0.89	0.519	0.69	446
17	0.90	0.523	0.68	525
18	0.98	0.513	0.63	446
19	1.02	0.530	0.37	336
20	1.02	0.508	0.64	423
21	1.07	0.510	0.39	388
22	1.11	0.496	0.52	388
23	1.19	0.500	0.69	532
24	1.21	0.499	0.43	308
25	1.28	0.505	0.50	369
26	1.30	0.521	0.48	353
27	1.30	0.560	0.45	398
28	1.43	0.507	0.39	279
29	1.48	0.539	0.58	473
30	1.60	0.515	0.42	343
31	1.66	0.511	0.69	(46)

A1. Tensile properties of GD0.5 (continued).

32	1.67	0.555	0.57	428
33	1.80	0.515	0.44	317
34	1.89	0.507	0.36	302
35	1.98	0.530	0.41	359
36	2.04	0.519	0.43	335
37	2.15	0.528	0.42	341
38	2.25	0.523	0.32	229
39	2.36	0.530	0.37	264
40	2.49	0.512	0.37	268
41	2.81	0.525	0.36	246
42	2.98	0.560	0.35	205
43	3.70	0.530	0.27	185

A2: Tensile properties of GD1.0.

Specimen #	c (mm)	Thickness (mm)	σ_{bc} (MPa)	ε_{bc} (%)
1	0.11	0.540	6.91	812
2	0.13	0.537	7.88	782
3	0.16	0.548	5.21	730
4	0.25	0.571	3.69	685
5	0.28	0.522	5.41	761
6	0.29	0.520	5.24	906
7	0.32	0.523	4.92	789
8	0.36	0.579	4.50	704
9	0.37	0.612	3.71	717
10	0.42	0.539	4.13	766
11	0.43	0.579	5.13	731
12	0.44	0.529	4.25	764
13	0.49	0.573	4.01	736
14	0.53	0.583	2.86	640
15	0.56	0.577	3.76	699
16	0.63	0.533	2.82	697
17	0.68	0.569	3.51	703
18	0.73	0.532	3.15	693
19	0.77	0.580	1.20	462
20	0.77	0.532	2.69	648
21	0.79	0.536	2.47	665
22	0.92	0.535	2.00	629
23	0.98	0.541	1.00	371
24	1.03	0.523	1.00	478
25	1.03	0.543	1.84	691
26	1.08	0.536	0.84	414
27	1.09	0.555	1.22	621
28	1.15	0.495	1.39	501
29	1.28	0.535	1.30	554
30	1.44	0.537	0.88	535
31	1.50	0.520	0.83	437
32	1.57	0.522	0.93	444
33	1.63	0.537	0.55	294
34	1.80	0.529	0.77	369
35	1.96	0.547	0.61	294
36	2.33	0.489	0.55	266
37	2.50	0.541	0.61	281
38	2.53	0.523	0.71	344
39	2.78	0.511	0.47	207
40	2.94	0.545	0.59	275

A3: Tensile properties of GD1.55.

Specimen #	c (mm)	Thickness (mm)	σ_{bc} (MPa)	ε_{bc} (%)
1	0.19	0.563	6.42	671
2	0.25	0.581	6.07	644
3	0.25	0.537	8.32	719
4	0.32	0.549	6.61	664
5	0.36	0.553	5.70	636
6	0.39	0.628	6.50	642
7	0.43	0.611	7.26	677
8	0.44	0.563	5.44	625
9	0.48	0.593	5.64	641
10	0.50	0.564	5.25	648
11	0.59	0.567	4.24	633
12	0.64	0.553	4.71	644
13	0.70	0.571	3.46	872
14	0.70	0.559	3.82	614
15	0.71	0.575	3.38	584
16	0.76	0.550	4.27	620
17	0.78	0.583	3.09	563
18	0.80	0.566	3.88	952
19	0.84	0.558	3.99	607
20	0.87	0.576	3.98	954
21	0.89	0.555	3.01	579
22	0.97	0.573	2.83	547
23	1.00	0.568	2.88	818
24	1.06	0.567	2.86	563
25	1.10	0.574	2.58	521
26	1.12	0.554	1.31	413
27	1.18	0.570	1.08	344
28	1.19	0.575	2.29	537
29	1.29	0.564	1.47	415
30	1.29	0.567	2.07	674
31	1.33	0.559	1.69	459
32	1.38	0.575	1.07	399
33	1.41	0.561	1.19	351
34	1.54	0.587	1.91	601
35	1.58	0.571	1.28	408
36	1.62	0.545	0.84	289
37	1.83	0.563	1.09	385
38	1.89	0.564	1.64	514
39	1.89	0.575	1.26	388
40	1.92	0.571	1.23	436
41	1.92	0.544	0.98	317
42	1.97	0.565	1.50	453

A3. Tensile properties of GD1.55 (continued).

43	2.10	0.555	0.73	228
44	2.18	0.574	0.68	235
45	2.27	0.543	1.14	355
46	2.46	0.571	1.25	431
47	2.76	0.573	0.70	239
48	2.98	0.565	0.83	305
49	3.39	0.606	0.54	154

A4. Tensile properties of GD1.8.

Specimen #	c (mm)	Thickness (mm)	σ_{bc} (MPa)	ε_{bc} (%)
1	0.19	0.563	6.42	671
2	0.25	0.581	6.07	644
3	0.25	0.537	8.32	719
4	0.32	0.549	6.61	664
5	0.36	0.553	5.70	636
6	0.39	0.628	6.50	642
7	0.43	0.611	7.26	677
8	0.44	0.563	5.44	625
9	0.48	0.593	5.64	641
10	0.50	0.564	5.25	648
11	0.59	0.567	4.24	633
12	0.64	0.553	4.71	644
13	0.70	0.571	3.46	872
14	0.70	0.559	3.82	614
15	0.71	0.575	3.38	584
16	0.76	0.550	4.27	620
17	0.78	0.583	3.09	563
18	0.80	0.566	3.88	952
19	0.84	0.558	3.99	607
20	0.87	0.576	3.98	954
21	0.89	0.555	3.01	579
22	0.97	0.573	2.83	547
23	1.00	0.568	2.88	818
24	1.06	0.567	2.86	563
25	1.10	0.574	2.58	521
26	1.12	0.554	1.31	413
27	1.18	0.570	1.08	344
28	1.19	0.575	2.29	537
29	1.29	0.564	1.47	415
30	1.29	0.567	2.07	674
31	1.33	0.559	1.69	459
32	1.38	0.575	1.07	399
33	1.41	0.561	1.19	351
34	1.54	0.587	1.91	601
35	1.58	0.571	1.28	408
36	1.62	0.545	0.84	289
37	1.83	0.563	1.09	385
38	1.89	0.564	1.64	514
39	1.89	0.575	1.26	388
40	1.92	0.571	1.23	436
41	1.92	0.544	0.98	317
42	1.97	0.565	1.50	453

A5. Tensile properties of GD2.0.

Specimen #	c (mm)	Thickness (mm)	σ_{bc} (MPa)	ε_{bc} (%)
1	0.10	0.531	15.6	740
2	0.12	0.534	10.0	669
3	0.14	0.538	11.4	676
4	0.17	0.533	7.30	620
5	0.17	0.520	8.99	627
6	0.23	0.529	7.36	611
7	0.29	0.551	7.73	650
8	0.35	0.565	5.53	594
9	0.44	0.535	5.25	594
10	0.48	0.549	3.87	636
11	0.48	0.573	3.96	579
12	0.49	0.561	5.59	674
13	0.60	0.545	4.14	576
14	0.61	0.555	4.37	557
15	0.68	0.631	2.82	528
16	0.73	0.567	1.11	292
17	0.73	0.491	2.15	473
18	0.77	0.642	1.79	418
19	0.82	0.550	1.13	300
20	0.83	0.552	3.31	621
21	0.87	0.557	3.09	578
22	0.88	0.550	3.51	632
23	1.01	0.577	3.22	550
24	1.11	0.597	1.46	355
25	1.11	0.569	1.11	275
26	1.17	0.589	0.96	253
27	1.18	0.542	1.01	275
28	1.30	0.586	1.02	262
29	1.38	0.573	1.03	278
30	1.39	0.502	1.18	283
31	1.39	0.568	1.03	282
32	1.54	0.540	0.89	254
33	1.63	0.581	0.76	192
34	1.64	0.570	0.75	194
35	1.70	0.555	0.87	238
36	1.73	0.570	1.06	308
37	1.98	0.483	0.61	146
38	2.15	0.562	0.67	159
39	2.33	0.501	0.69	177
40	2.39	0.576	0.76	218
41	2.66	0.529	0.64	185
42	2.66	0.583	0.58	133

A5. Tensile properties of GD2.0 (continued).

43	3.05	0.554	0.59	157

A6. Tensile properties of GD2.5.

Specimen #	c (mm)	Thickness (mm)	σ_{bc} (MPa)	ε_{bc} (%)
1	0.12	0.563	11.4	706
2	0.13	0.574	11.1	631
3	0.15	0.597	10.2	600
4	0.19	0.569	12.4	612
5	0.20	0.568	11.9	701
6	0.24	0.559	11.6	723
7	0.29	0.603	8.62	574
8	0.31	0.586	8.45	-94
9	0.38	0.576	7.02	570
10	0.52	0.573	5.37	532
11	0.58	0.565	5.04	495
12	0.62	0.570	5.20	827
13	0.63	0.568	5.49	879
14	0.69	0.555	4.03	583
15	0.82	0.597	4.48	502
16	0.85	0.595	3.53	581
17	0.93	0.575	1.50	317
18	0.94	0.579	3.03	464
19	1.02	0.585	2.64	518
20	1.08	0.575	2.79	521
21	1.13	0.572	2.54	508
22	1.20	0.606	1.14	232
23	1.20	0.577	1.04	217
24	1.27	0.583	0.89	168
25	1.41	0.588	1.06	223
26	1.49	0.600	1.05	234
27	1.58	0.594	0.91	198
28	1.74	0.586	1.19	276
29	1.82	0.561	0.94	223
30	1.94	0.587	0.76	158
31	2.07	0.571	1.11	269
32	2.16	0.579	0.96	214
33	2.30	0.567	1.09	255
34	2.31	0.573	0.92	209
35	2.50	0.571	1.11	261
36	2.75	0.576	0.62	117
37	3.00	0.587	0.89	205

A7. Tensile properties of GD3.0.

Specimen #	c (mm)	Thickness (mm)	σ_{bc} (MPa)	ε_{bc} (%)
1	0.10	0.535	15.7	611
2	0.13	0.563	11.2	640
3	0.16	0.543	8.38	922
4	0.16	0.549	13.0	-70
5	0.24	0.556	6.91	597
6	0.28	0.535	6.96	830
7	0.32	0.541	5.52	715
8	0.34	0.576	6.38	604
9	0.36	0.555	5.44	585
10	0.43	0.554	4.63	560
11	0.52	0.553	4.35	552
12	0.59	0.543	3.78	652
13	0.67	0.555	3.45	613
14	0.71	0.557	1.94	290
15	0.73	0.558	1.43	263
16	0.77	0.568	1.29	193
17	0.82	0.549	2.62	472
18	0.89	0.555	1.45	242
19	0.98	0.579	1.08	171
20	1.10	0.581	1.77	293
21	1.24	0.578	1.15	188
22	1.42	0.591	1.37	221
23	1.49	0.566	1.20	195
24	1.53	0.595	1.05	168
25	1.57	0.566	1.16	159
26	1.69	0.565	1.19	183
27	1.71	0.575	0.87	120
28	1.80	0.573	0.91	118
29	1.86	0.574	0.90	115
30	2.02	0.571	1.09	157
31	2.15	0.559	0.94	129
32	2.45	0.567	0.85	117
33	2.70	0.563	0.73	86
34	2.75	0.587	0.62	69
35	2.79	0.561	0.73	90
36	2.91	0.569	1.02	169

A8. Tensile properties of GD4.0 (continued).

Specimen #	c (mm)	Thickness (mm)	σ_{bc} (MPa)	ε_{bc} (%)
1	0.107	0.582	13.5	508
2	0.127	0.561	11.4	483
3	0.150	0.556	7.84	785
4	0.153	0.549	6.67	654
5	0.162	0.581	4.31	385
6	0.177	0.577	7.06	562
7	0.197	0.545	5.68	416
8	0.212	0.540	5.10	427
9	0.212	0.593	4.92	483
10	0.218	0.599	7.49	682
11	0.257	0.540	6.11	430
12	0.262	0.567	1.51	191
13	0.277	0.569	7.38	450
14	0.295	0.562	5.04	419
15	0.310	0.595	4.56	574
16	0.310	0.589	1.31	159
17	0.317	0.553	5.03	412
18	0.328	0.547	4.71	657
19	0.340	0.566	1.30	175
20	0.378	0.557	2.18	294
21	0.413	0.563	1.26	171
22	0.440	0.558	1.26	166
23	0.445	0.579	1.98	251
24	0.500	0.537	1.18	138
25	0.515	0.569	1.78	223
26	0.567	0.552	1.08	136
27	0.572	0.569	1.16	158
28	0.592	0.551	2.74	384
29	0.683	0.563	1.53	191
30	0.802	0.558	1.61	212
31	0.833	0.585	1.09	152
32	0.888	0.580	1.41	186
33	1.007	0.570	0.82	94
34	1.167	0.561	0.89	99
35	1.177	0.590	1.19	164
36	1.387	0.547	0.91	105
37	1.402	0.573	0.82	98
38	1.560	0.569	1.03	138
39	1.650	0.565	0.77	80
40	1.973	0.573	0.68	66
41	2.203	0.567	0.61	57
42	2.227	0.565	0.68	73

A8. Tensile properties of GD4.0 (continued).

43	2.370	0.617	0.74	94
44	2.753	0.559	0.71	81
45	3.217	0.551	0.65	77

A9. Tensile properties of GD5.0 (continued).

Specimen #	c (mm)	Thickness (mm)	σ_{bc} (MPa)	ε_{bc} (%)
1	0.113	0.571	6.19	352
2	0.118	0.583	7.79	562
3	0.128	0.568	2.12	203
4	0.137	0.540	2.58	255
5	0.153	0.561	1.16	106
6	0.158	0.563	1.89	190
7	0.162	0.545	2.30	223
8	0.173	0.556	2.77	247
9	0.178	0.570	1.33	127
10	0.190	0.559	1.44	141
11	0.200	0.531	2.32	228
12	0.203	0.574	1.33	127
13	0.213	0.560	1.22	115
14	0.242	0.567	2.18	212
15	0.272	0.559	1.70	168
16	0.298	0.556	1.46	153
17	0.365	0.580	1.58	157
18	0.468	0.573	1.10	102
19	0.495	0.581	1.36	134
20	0.618	0.564	0.92	80
21	0.780	0.559	1.23	122
22	0.925	0.593	1.00	84
23	1.095	0.561	0.92	84
24	1.102	0.595	0.74	57
25	1.178	0.583	0.73	50
26	1.237	0.615	0.72	54
27	1.373	0.577	0.76	62
28	1.542	0.593	0.64	44
29	1.655	0.615	0.61	45
30	1.668	0.620	0.59	40
31	1.723	0.568	0.59	43
32	1.840	0.615	0.69	54
33	1.898	0.588	0.63	51
34	2.050	0.586	0.67	55
35	2.298	0.614	0.63	48
36	2.403	0.615	0.55	39
37	2.542	0.568	0.64	50
38	2.657	0.583	0.59	47
39	3.023	0.612	0.48	33

A10. Tensile properties of G6.0 (continued).

Specimen #	c (mm)	Thickness (mm)	σ_{bc} (MPa)	ε_{bc} (%)
1	0.11	0.599	1.80	166
2	0.13	0.545	1.66	158
3	0.17	0.533	1.95	191
4	0.20	0.586	1.28	110
5	0.25	0.549	1.20	104
6	0.31	0.573	0.96	73
7	0.40	0.601	1.00	78
8	0.40	0.550	0.86	64
9	0.48	0.598	0.77	53
10	0.57	0.591	0.81	57
11	0.60	0.635	0.68	45
12	0.70	0.587	0.71	48
13	0.74	0.600	0.82	53
14	0.81	0.597	0.82	55
15	0.92	0.603	0.83	66
16	0.99	0.583	0.65	39
17	1.05	0.544	0.61	40
18	1.11	0.588	0.61	30
19	1.20	0.610	0.45	22
20	1.31	0.588	0.72	53
21	1.53	0.589	0.51	30
22	1.58	0.553	0.53	33
23	1.64	0.595	0.59	37
24	1.78	0.649	0.52	30
25	1.87	0.646	0.48	29
26	1.91	0.606	0.63	46
27	1.98	0.607	0.45	23
28	1.99	0.530	0.46	26
29	2.32	0.589	0.41	22
30	2.38	0.598	0.37	20
31	2.40	0.589	0.41	23
32	2.74	0.605	0.42	27
33	2.85	0.605	0.46	34
34	2.89	0.603	0.45	27
35	2.95	0.603	0.46	31